

Copyright Warning & Restrictions

The copyright law of the United States (Title 17, United States Code) governs the making of photocopies or other reproductions of copyrighted material.

Under certain conditions specified in the law, libraries and archives are authorized to furnish a photocopy or other reproduction. One of these specified conditions is that the photocopy or reproduction is not to be “used for any purpose other than private study, scholarship, or research.” If a user makes a request for, or later uses, a photocopy or reproduction for purposes in excess of “fair use” that user may be liable for copyright infringement,

This institution reserves the right to refuse to accept a copying order if, in its judgment, fulfillment of the order would involve violation of copyright law.

Please Note: The author retains the copyright while the New Jersey Institute of Technology reserves the right to distribute this thesis or dissertation

Printing note: If you do not wish to print this page, then select “Pages from: first page # to: last page #” on the print dialog screen

The Van Houten library has removed some of the personal information and all signatures from the approval page and biographical sketches of theses and dissertations in order to protect the identity of NJIT graduates and faculty.

ABSTRACT

STUDY OF CONTROLLED RELEASE OF DAPSONE FROM MODIFIED MONTMORILLONITE AND POLYMER MATRICES

by
Jia Fan

This thesis focuses on the controlled release system of Dapsone (DAP) as the Active Pharmaceutical Ingredient (API) intercalated into sodium montmorillonite (MMT- Na^+) and their combination with an anionic copolymer (Eudragit[®] S100). The effects of the excipients on the API dissolution rate were studied from their release profile in simulated intestinal fluid (pH=7.4) at 37 ± 0.5 °C. In the first part of the research, ionizable Dapsone was intercalated in the interlayers of MMT- Na^+ to produce a nanohybrid. In the second part of the research, the nanohybrid was melt dispersed in the polymer to produce ternary (API/ Clay/ Polymer) composites. For comparison, API-polymer solid dispersions were prepared by melt mixing in the absence of nanoclay.

The intercalated compound was characterized by X-ray diffraction (XRD), Fourier transform infrared (FT-IR) spectroscopy, and thermogravimetric analysis (TGA). The basal spacing of montmorillonite increased from 1.17nm to 1.55nm. The *in vitro* release experiments revealed that Dapsone was steadily released from MMT. In the second part of the research, an API-polymer miscible system was prepared by melt mixing. In agreement with solubility parameter differences, Dapsone exists in an amorphous state in the polymer matrix. The API-modified clay was dispersed in the polymer to form a ternary system, in which the API showed a more controlled release profile due to the presence of the nanoclay.

**STUDY OF CONTROLLED RELEASE OF DAPSONE FROM MODIFIED
MONTMORILLONITE AND POLYMER MATRICES**

**by
Jia Fan**

**A Thesis
Submitted to the Faculty of
New Jersey Institute of Technology
In Partial Fulfillment of the Requirements for the Degree of
Master of Science in Engineering**

**Otto H. York Department of
Chemical, Biological and Pharmaceutical Engineering**

January 2011

Blank Page

APPROVAL PAGE

**STUDY OF CONTROLLED RELEASE OF DAPSONE FROM MODIFIED
MONTMORILLONITE AND POLYMER MATRICES**

Jia Fan

Dr. Marino Xanthos, Thesis Advisor Date
Professor of Chemical, Biological and Pharmaceutical Engineering, NJIT

Dr. Laurent Simon, Committee Member Date
Associate Professor of Chemical, Biological and Pharmaceutical Engineering, NJIT

Dr. Ecevit A. Bilgili, Committee Member Date
Assistant Professor of Chemical, Biological and Pharmaceutical Engineering, NJIT

BIOGRAPHICAL SKETCH

Author: Jia Fan
Degree: Master of Science
Date: January 2011

Undergraduate and Graduate Education:

- Master of Science in Chemical Engineering,
New Jersey Institute of Technology, Newark, NJ, 2011
- Bachelor of Science in Polymer Science & Engineering,
Jilin Institute of Chemical Technology, Jilin, P. R. China, 2008

Major: Chemical Engineering

In memory of my little cousin – Amy Fan

ACKNOWLEDGMENT

First, I would like to acknowledge my advisor, Professor Marino Xanthos for his professional guidance, kind encouragement and financial support throughout this research. He also gave me many opportunities to enlarge my vision in my research area. His significant efforts in this project are highly appreciated and I will never forget this help.

I would like to thank my Committee members, Professor Laurent Simon and Professor Ecevit A. Bilgili for their advice and priceless support.

I would like to express my profound gratitude to my senior friend, Jin Uk Ha, who has already been back to Korea, but his invaluable assistance with my research really led me to succeed in lab experiments.

Moreover, I am grateful to my parents, my grandparents, my uncle's family and my girlfriend for their endless support during my graduate studies.

TABLE OF CONTENTS

Chapter	Page
1 INTRODUCTION.....	1
2 LITERATURE SURVEY.....	3
2.1 Compounds of Nanoclays with APIs.....	3
2.2 Compounds of Polymers with APIs.....	6
2.3 Compounds of Polymers with API-Intercalated Clays.....	10
3 EXPERIMENTAL.....	13
3.1 Materials.....	13
3.1.1 Active Pharmaceutical Ingredient.....	13
3.1.2 Cationic Nanoclay.....	14
3.1.3 Polymer Excipient.....	15
3.1.4 Plasticizer.....	16
3.2 Sample Preparation.....	16
3.2.1 Preparation of DAP Functionalized Clay.....	16
3.2.2 Preparation of Eudragit [®] S100/DAP and Eudragit [®] S-100/DAP/Clay Compounds by Melt Mixing.....	17
3.3 Characterization.....	17
3.3.1 Fourier Transform Infrared (TF-IR) Spectrophotometry.....	17
3.3.2 Wide Angle X-Ray Diffraction (WXRD).....	17
3.3.3 Thermogravimetric Analysis (TGA).....	18
3.3.4 Differential Scanning Calorimetry (DSC).....	18

TABLE OF CONTENTS
(Continued)

Chapter	Page
3.3.5 Scanning Electron Microscopy (SEM).....	18
3.3.6 Energy Dispersive X-Ray Analysis (EDX).....	19
3.3.7 Elemental Analysis.....	19
3.3.8 Dissolution Test and UV-Vis Analysis.....	19
4 DISCUSSION.....	20
4.1 Results on Clay Modified with Dapsone.....	20
4.1.1 FTIR Analysis.....	20
4.1.2 XRD Analysis.....	21
4.1.3 Thermal Analysis.....	23
4.1.4 Quantitative Analysis of MMT-DAP.....	24
4.1.5 Dissolution Test.....	25
4.2 Results on DAP Compounded with Eudragit®S100.....	26
4.2.1 Thermal Analysis.....	26
4.2.2 XRD Analysis.....	28
4.2.3 Morphology.....	29
4.2.4 Dissolution Test.....	31
4.3 Results on DAP modified Clay Compounded with Eudragit®S100.....	33
4.3.1 Thermal Analysis.....	33
4.3.2 XRD Analysis.....	35
4.3.3 Morphology.....	36

TABLE OF CONTENTS
(Continued)

Chapter	Page
4.3.4 Dissolution Test.....	41
5 CONCLUSIONS.....	43
APPENDIX A CALCULATION OF API CONTENT IN NANOCCLAY	45
APPENDIX B CALCULATION OF SOLUBILITY PARAMETERS.....	46
APPENDIX C INTERCALATION STUDY.....	48
REFERENCES	56

LIST OF TABLES

Table	Page
4.1 Results of MMT-DAP Elemental Analysis.....	25
B.1 Hildebrand Solubility Parameters of Dapsone Groups.....	46
B.2 Hildebrand Solubility Parameters of Eudragit® S100 Groups.....	46
C.1 Abbreviations of MMT-Na ⁺ Samples Modified with Dapsone.....	48

LIST OF FIGURES

Figure	Page
2.1 Amorphous solid solution.....	6
3.1 Chemical structure of Dapsone.....	13
3.2 Molecular structure of MMT-Na ⁺	14
3.3 Chemical structure of Eudragit [®] S-100.....	15
3.4 Chemical structure of triethyl citrate.....	16
4.1 FTIR results of (a) Dapsone (DAP), (b) MMT-DAP, and (c) MMT-Na ⁺	21
4.2 XRD results of (a) Dapsone, (b) MMT-Na ⁺ , and (c) MMT-DAP.....	22
4.3 TGA results of (a) MMT-Na ⁺ , (b) MMT-DAP, and (c) Dapsone.....	23
4.4 DSC results of MMT-Na ⁺ , MMT-DAP, and Dapsone.....	24
4.5 Dissolution results in simulated intestinal fluid (phosphate buffer pH=7.4) of (a) Dapsone and (b) MMT-DAP.....	25
4.6 TGA results of (a) Dapsone, (b) Eudragit [®] S100, (c) TEC, (d) Eudragit [®] S100/ 20wt% TEC, (e) Eudragit [®] S100/ 20wt% TEC-5wt% DAP, and (f) Eudragit [®] S100/ 20wt% TEC-10wt% DAP.....	27
4.7 T _g of (a) Eudragit [®] S100, (b) Eudragit [®] S100/ 20wt% TEC, (c) Eudragit [®] S100/ 20wt% TEC-5wt% DAP, and (d) Eudragit [®] S100/ 20wt% TEC-10wt% DAP.....	28
4.8 XRD results of (a) Eudragit [®] S100/ 20wt% TEC, (b) Eudragit [®] S100/ 20wt% TEC-10wt% DAP, (c) Eudragit [®] S100/ 20wt% TEC-5wt% DAP, and (d) Dapsone.....	29
4.9 Polarized optical microscopy image of Eudragit [®] S100/ 20wt% TEC-10wt% DAP.....	30
4.10 SEM image of Eudragit [®] S100/ 20wt% TEC-10wt% DAP (left) and EDX sulfur mapping image of the same region (right).....	30

**LIST OF FIGURES
(Continued)**

Figure	Page
4.11 Dissolution results in simulated intestinal fluid (phosphate buffer pH=7.4) of (a) Dapsone, (b) Eudragit [®] S100/ 20wt% TEC-5wt% DAP and (c) Eudragit [®] S100/ 20wt% TEC-10wt% DAP.....	31
4.12 TGA results of (a) Eudragit [®] S100/ 20wt% TEC, (b) Eudragit [®] S100/ 20wt% TEC-10wt% DAP, (c) Eudragit [®] S100/ 20wt% TEC-10wt% (DAP/MMT-Na ⁺ physical mixture), and (d) Eudragit [®] S100/ 20wt% TEC-10wt% (MMT-DAP hybrid).....	33
4.13 T _g of (a) Eudragit [®] S100, (b) Eudragit [®] S100/ 20wt% TEC-10wt% DAP, (c) Eudragit [®] S100/ 20wt% TEC-10wt% (DAP/MMT-Na ⁺ physical mixture), and (d) Eudragit [®] S100/ 20wt% TEC-10wt% (MMT-DAP hybrid).....	34
4.14 XRD results of (a) Eudragit [®] S100/ 20wt% TEC-10wt% DAP, (b) MMT-Na ⁺ , and (c) MMT-DAP, (d) Eudragit [®] S100/ 20wt% TEC-10wt% (MMT-DAP hybrid), and (e) Eudragit [®] S100/ 20wt% TEC-10wt% (DAP/MMT-Na ⁺ physical mixture).....	35
4.15 SEM image of 10wt% DAP/MMT-Na ⁺ physical mixture in Eudragit [®] S100 and EDX mappings of elements aluminum, silicon, sodium and sulfur.....	37
4.16 SEM image of 10wt% DAP/MMT-Na ⁺ physical mixture in Eudragit [®] S100 and EXD Mapping of aluminum (left) and silicon (right).....	38
4.17 Magnified SEM images of circle shown in Figure 4.16.....	39
4.18 SEM image of 10wt% MMT-DAP hybrid in Eudragit [®] S100 and EDX mappings of elements aluminum, silicon and sulfur.....	40
4.19 Dissolution results in simulated intestinal fluid (phosphate buffer pH=7.4) of (a) Eudragit [®] S100/ 20wt% TEC-10wt% DAP, (b) Eudragit [®] S100/ 20wt% TEC-10wt% (DAP/MMT-Na ⁺ physical mixture), and (c) Eudragit [®] S100/ 20wt% TEC-10wt% (MMT-DAP hybrid).....	41
C.1 XRD results of Dapsone, MMT-Na ⁺ , (a) 2xRT24h-N and (b) 2xRT24h.....	49

LIST OF FIGURES
(Continued)

Figure	Page
C.2 TGA results of Dapsone, MMT-Na ⁺ , (a) 2xRT24h-N and (b) 2xRT24h.....	50
C.3 Weight loss of MMT-DAP hybrids soaked in different times.....	51
C.4 XRD results of (b) 2xRT24h, (c) 2xRT15h, (d) 2xRT3h and (e) 2xRT1h.....	52
C.5 Intercalation of Dapsone at different temperatures.....	53
C.6 XRD results of (d) 2xRT3h, (e) 2xRT1h, (f) 2x60°C3h and (g) 2x60°C1h.....	54
C.7 TGA results of (e) 2xRT1h and (h) 1xRT1h	54

CHAPTER 1

INTRODUCTION

Drug bioavailability implies the extent and rate at which a drug becomes available in the general circulation. Dissolution of the drug in the aqueous gastric and intestinal surroundings is a requirement for its absorption following oral administration.¹ Based on their solubility and intestinal permeability characteristics, drug substances have been classified into four categories according to the Biopharmaceutics Classification System (BCS) proposed by Amidon et al.²

BCS class II drugs exhibit low solubility and high permeability characteristics. Their oral absorption is mostly governed by *in vivo* dissolution³; solubility behavior is a key determinant for the oral bioavailability of these drugs.⁴ Dapsone (DAP), a symmetric drug with two identical aromatic amine groups, belongs to the BCS class II.⁵ To improve oral bioavailability of such poorly water soluble drugs, different techniques can be used, such as salt formation, particle size reduction and solid dispersion.⁶ In this thesis, three different types of drug delivery systems prepared by different methods are investigated.

Montmorillonite (MMT) is a biocompatible natural clay mineral that has already found uses in pharmaceutical applications. Its layer structure has a superior capability to intercalate large molecules into the interlayer space. In this research, the intercalation of Dapsone into montmorillonite as drug carrier was firstly investigated. Generally, intercalation of API in MMT is a fast process, due to the occurrence of an ion exchange reaction between the interlayer Na^+ ions and cationic API molecules.⁷ Dapsone release from the MMT-DAP hybrid in simulated intestinal fluid was subsequently investigated.

Preparation of an amorphous solid dispersion in polymers is another effective way of increasing the dissolution rate of poorly water-soluble drugs, which is also the purpose of the second part of this research. Hot melt extrusion (HME) is currently being investigated for applications in pharmaceutical dosage development to produce polymer/API solid dispersions;⁸ it is a solvent free continuous process that can lead to fewer processing steps. In this study, a batch mixer was used for the small scale melt mixing process since it has two counter-rotating screws, which impart mixing similar to that generated by twin-screw extruders.⁹ Eudragit[®] S100, an amorphous copolymer showing complete dissolution at pH greater than 7, was selected in this investigation. By calculating solubility parameters, the miscibility of Dapsone in the polymer matrix can be predicted and subsequently confirmed by the morphology of the compounds.

The last part of this research refers to a novel delivery system containing MMT-DAP hybrid dispersed in Eudragit[®] S100 matrix by the melt mixing process. Compared with the polymer/API system, this ternary system is anticipated to achieve a more controllable and/or sustained API release pattern since the API intercalated nanoclay combined with the slow diffusion of the polymer would result in a more tortuous path for API release. This has been demonstrated in an equivalent system containing an anionic clay-anionic API nanohybrid, with or without a polymer.¹⁰ In order to understand and identify potential pharmaceutical applications of this ternary system for controlled drug delivery, a physical mixture of MMT and Dapsone was also mixed with Eudragit[®] S100 as a comparison. Furthermore, miscibility and thermal stability of the polymer/hybrid mixture produced by intercalation or mechanical blending are investigated.

CHAPTER 2

LITERATURE SURVEY

2.1 Compounds of Nanoclays with APIs

Clay minerals have large specific surface area and exhibit good adsorbability, ion exchange capacity, standout adhesive ability and drug carrying capability.¹¹ Clays play an important role in pharmaceutical products used as excipients and active agents. Hydrotalcite (HT), also known as layered double hydroxides (LDH), is an anionic nanoclay with positively charged layers and charge-balancing anions in the interlayer space.¹² Montmorillonite (MMT) is one mineral of the smectite group, composed of silica tetrahedral sheets layered between alumina octahedral sheets. The imperfection of the crystal lattice induces a net negative charge that leads to the adsorption of alkaline earth metal ions in the interlayer space.⁷ The clays intercalated by API as drug carrier have received considerable attention in recent years. Some commercialized pharmaceutical products using clay minerals as excipients are currently sold in the market.¹²

Zhang et al.¹³ investigated the intercalation of Captopril into the interspacing of LDH followed by its release which was carried out in a simulated gastrointestinal and intestinal fluid at pH 4.60 and 7.45 as release medium. The intercalation of the anionic clay was confirmed by TG-DTA, XRD and FT-IR. Approximately 31.11% of Captopril was intercalated into the interspace, and as result the interlayer distance increased from 0.48 nm to 1.462 nm. *In vitro* drug release studies showed that the release rate and release percentages of API from the hybrid were markedly decreased with increasing medium pH value.

Xia et al.¹⁴ intercalated several anionic antihypertensive drugs including Enalapril, Lisinopril, Captopril and Ramipril into Zn/Al layered double hydroxides; the intercalations were verified by observing XRD peak shifting to low 2θ angles indicating a swelling of the layers due to the drug molecules. Calculated drug loading in the Zn-Al LDHs interspace ranged from 28.79% to 47.22%. The sustained-release profiles of API from drug-LDHs followed the Higuchi's square root law because the concentration of API release increased with the square root of time.

Controlled drug release of ibuprofen (IBU) intercalated in montmorillonite was investigated by Zheng et al.¹⁵ According to XRD and TGA results, the basal spacing of montmorillonite increased from 1.25 nm to 1.57 nm and the decomposition temperature of intercalated IBU was increased to 471 °C. From FT-IR results, several new absorption bands were recognized and indicated that IBU interacts strongly with the montmorillonite layers. The *in vitro* release experiment showed that the release of IBU from IBU/MMT hybrid was affected by the pH value. The release rate in simulated intestinal fluid (pH=7.4) was noticeably higher than that in simulated gastric fluid (pH=1.2).

Lin et al.¹⁶ studied purified montmorillonite intercalated with 5-fluorouracil (5-FU) as drug carrier. The optimum condition for 5-FU/montmorillonite preparations is 1.185% of 5-FU as initial concentration under a pH value of 11.6 at a temperature of 80 °C and a soaking time of 2h. From FTIR, TGA and XRD data, 5-FU has been confirmed to successfully intercalate into the interlayers of montmorillonite both by free surface adsorption and sodium ion replacement. The composite of 5-FU/montmorillonite is expected to achieve *in situ* release for colorectal cancer therapy in future applications.

Joshi et al.⁷ reported that the intercalation of timolol maleate (TM) into MMT was a rapid process and equilibrium was attained within 1h. The maximum amount of TM intercalated into MMT is 217 mg/g MMT within 1h at pH 5.7 and 30 °C. Intercalation of TM into MMT depends on the pH of the interaction medium. XRD patterns of the hybrid material showed an increase in the *d*-spacing, conforming to the intercalation of TM into the interlayer of MMT. TG-DTA of MMT-TM showed a sharp weight loss at about 200 °C due to decomposition of exchanged TM. *In vitro* release study showed that about 43 and 48% of TM was released from the MMT-TM hybrid in simulated gastric fluid (pH 1.2) and intestinal fluid (pH 7.4), respectively. These studies indicate that MMT can be used as the sustained release carrier of TM in oral administration.

A study on the controlled release and antibacterial activity of chlorhexidine (CA) intercalated in montmorillonite was reported by Meng et al.¹⁷ The XRD patterns of CA/MMT showed an expansion in the clay basal spacing indicating that CA was intercalated into the interlayer of MMT. In a drug release study of CA/MMT, CA was burst released for the initial 24 hours and then was continuously released over 72 hours. Therefore, MMT was suggested as an advanced drug delivery carrier with controlled release characteristics. The antibacterial activity of CA/MMT was evaluated by the inhibitory zone tests. The results showed that CA/MMT composites had broad-spectrum antibacterial capability.

2.2 Compounds of Polymers with APIs

Binary polymer-API systems are usually desired to be miscible if, after a given processing operation such as hot melt extrusion or solvent evaporation, only one glass transition temperature exists. The amorphous form of API may provide enhanced solubility, dissolution rate, and bioavailability but will also potentially crystallize over time.¹⁸ More recently, many polymers including polyvinylpyrrolidone (PVP), polyethyleneoxide (PEO), Eudragit (acrylates), polyethylene glycol (PEG) and cellulose derivatives have been reported for being used as drug carriers. These polymers are particularly likely to form amorphous solid solutions as the polymers are present in the form of amorphous polymer chain networks (Figure 2.1). In addition, the API molecules as solutes can plasticize the polymer, leading to a reduction in its glass transition temperature. With respect to the HME technique, Forster et al.⁸ indicated that an important variable in the melt mixing process is the selection of a temperature that fully plasticizes the polymer without causing chemical decomposition of the API.

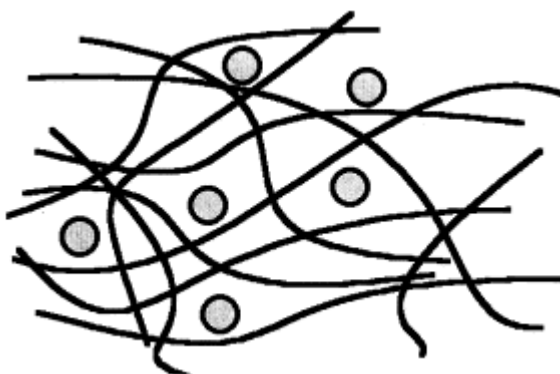


Figure 2.1 Amorphous solid solution.⁴

In order to select suitable combinations of polymers and APIs to form an amorphous solid solution, the miscibility in solid solution can be predicted by comparing the solubility parameters (δ) of polymers and APIs. The solubility parameter is defined as the square root of the cohesive energy density as described by equation¹⁹:

$$\delta = (\Delta E_v / V_m)^{0.5} \quad (2.1)$$

where ΔE_v represents the energy of vaporization and V_m is the molar volume of the material. The Hildebrand solubility parameters of the materials were calculated with the method proposed by Fedors²⁰:

$$\delta = (\sum \Delta e_i / \sum v_i)^{0.5} \quad (2.2)$$

where e_i and v_i are the additive atomic and group contributions for the energy of vaporization and the molar volume. Compounds with similar values for solubility parameters are likely to be miscible. This is because the energy of mixing within the components is balanced by the energy released by interaction between the components²¹. Greenhalgh²² demonstrated that compounds with $\Delta\delta < 7.0 \text{MPa}^{1/2}$ are likely to be miscible while compounds with $\Delta\delta > 10.0 \text{MPa}^{1/2}$ are likely to be immiscible.

Sun et al.⁶ studied the effects of nimodipine (NMD) on Eudragit[®] E100 (aminoacryl methacrylate copolymer) and Plasdone[®] S630 (vinyl pyrrolidone-vinyl acetate copolymer) prepared by hot melt extrusion. X-ray diffraction and DSC analysis showed that Eudragit[®] E100 and Plasdone[®] S630 were compatible with NMD in the solid dispersion system. HME was applied to disperse drugs to a molecular level in a given matrix. Compared with the pure drug and physical mixture, the dissolution of NMD was enhanced dramatically since the API was effectively transformed into an amorphous state.

Albers et al.²³ studied the poorly water-soluble drug celecoxib blended with a polymethacrylate carrier by hot-melt extrusion. XRD and DSC measurements indicated the formation of a glassy solid solution, where the drug is molecularly dispersed in the carrier. The amorphous state of the glassy solid solution could be maintained during the exposure to a mechanical stress in a milling process. Two mechanisms of drug release from solid dispersions were reviewed. Carrier-controlled dissolution predominates when the API release is dependent on the properties of the carrier. If the API release is dependent on the API properties it is called API-controlled dissolution. Solid-state properties and SEM images of extrudates after dissolution indicated that a carrier-controlled dissolution occurred in this system. Furthermore, recrystallization could be inhibited by the external addition of hydroxypropyl methylcellulose (HPMC) to the dissolution medium.

Mididoddi et al.²⁴ used hydroxypropyl cellulose (HPC) and poly(ethylene oxide) as polymer carrier and demonstrated that drug loaded films containing up to 20% ketoconazole were successfully prepared by HME processing. DSC, SEM and XRD techniques indicated that melt cooled mixtures of the drug and the two polymers were amorphous. The bioadhesive properties of these films were investigated on the human nail (*ex vivo*) using a Texture Analyzer[®], which could be influenced by instrument variables such as contact force, contact time and speed of probe removal from the tissue. The peak adhesion force (PAF) is the maximum force required to remove the extruded film from the human nail and the work of adhesion was determined from the area under the force-distance curve (AUC). In this study, higher PAF and AUC was achieved

indicating strong adhesive bonds between the HME film and nail, and this film would be relevant as potential dosage form for onychomycosis and other fungal infections.

Hot-melt extruded tablets with enteric and sustained-release properties were prepared by Yang et al.²⁵ using ketoprofen as a model drug and Eudragit® L100 as the carrier. Ketoprofen homogeneously dispersed in the polymer matrix in a non-crystalline state, and this was confirmed by DSC, XRD and SEM analysis. The drug release percentage was below 3% in 0.1M HCl and a sustained release for 6 to 12 hours was obtained with the tablets prepared by direct cutting of the extrudates and by compressing the pulverized extrudates, while no enteric and sustained-release properties were exhibited by the physical mixture tablets. For the cut tablets, the drug was released according to the erosion mechanism, whereas in the extruded tablets the release property was controlled by the erosion and diffusion mechanisms simultaneously.

Kakran et al.²⁶ used an evaporative precipitation of nanosuspension (EPN) method to fabricate composite particles of a poorly water-soluble antimalarial drug, artemisinin, with polyethylene glycol (PEG). The DSC and XRD studies suggested that the crystallinity of the EPN-prepared artemisinin decreased with increasing polymer concentration, which improved the dissolution of the artemisinin particles. The phase solubility of artemisinin increased linearly with increasing PEG concentration and temperature. The artemisinin/PEG composite particles produced by the EPN method have good potential for improved drug delivery in much smaller doses than with commercial preparation methods.

2.3 Compounds of Polymers with API-Intercalated Clays

Polymer-API intercalated nanoclay composites have recently been investigated for controlled drug release applications. Compared with polymer-API system, the compounds containing API modified clay minerals provide an advantageous drug delivery system. Because the release of API intercalated nanoclay is potentially controllable in pH dependent polymers as host matrices, these new materials have a great potential in the pharmaceutical field. There are only few reports on the API functionalized nanoclay compounded with polymer, especially using hot melt mixing process.

Ha¹⁰ reported this novel delivery system produced by hot melt mixing. Eudragit[®] E-100 containing 10 wt% sodium diclofenac (DIK) modified hydrotalcite was prepared by batch mixer at 50 rpm and 130 °C for 5 min. The XRD patterns of this ternary system showed crystalline peaks but were not same as those when Eudragit[®] E-100 was compounded with DIK; this may indicate that the DIK/clay still maintains its crystalline structure and no API was released during melt mixing. According to the morphology study that followed, Eudragit[®] E-100 mixed with DIK/clay showed better dispersion compared to the direct mixing of Eudragit[®] E-100 and DIK. Furthermore, DIK released from Eudragit[®] E-100-DIK/clay compound showed 10% higher solubility as compared to the polymer/API binary system. This could be attributed to the DIK present in amorphous state in the clay interlayer space.

Joshi et al.²⁷ illustrated the suitability of montmorillonite as a drug delivery carrier, by developing clay/API composite of ranitidine hydrochloride (RT) intercalated in MMT. The prepared MMT-RT hybrid was coated with cationic polymer Eudragit[®] E-100 by oil-

in-water solvent evaporation method. The interlayer spacing of 16.8Å for MMT-RT determined by XRD, suggested a vertical orientation of the RT cation in a bilayer arrangement. According to FT-IR analysis, the characteristic bands of RT shifted in the hybrid material signifying the strong interaction of RT into the MMT layers. *In vitro* release showed that 51% of RT was released from MMT-RT hybrid in gastric fluid of pH 1.2, which was greatly enhanced by coating with Eudragit[®] E-100. The release of RT from the hybrid followed the parabolic diffusion mechanism.

Li et al.²⁸ used an anti-inflammatory drug, fenbufen, intercalated with LDHs as the core followed by coating with Eudragit[®] S-100. The dissolution profile showed a slow release of the intercalated drug, but only 67% of the drug was liberated after 5 h at pH 7.4. This suggests that complete dissolution of the polymer and de-intercalation of fenbufen from the LDH may be inhibited by an interaction between the carboxylate groups of the polymer and the surface of the LDH.

Han et al.²⁹ reported that the intercalation of Paraquat (PQ), the cationic herbicide as a model compound used in the agricultural field, into the montmorillonite layers could be achieved by the ion exchange reaction and the simple solid state reaction, providing the controlled release functionality. According to the solid state reaction method, the mixture of Paraquat and MMT-Na⁺ was ground under 150 °C for 2 h. Compared with the hybrid prepared by the conventional solution reaction, there was no distinct difference in the XRD patterns, which showed the same expansion of basal spacing indicating that the PQ molecules were successfully intercalated into the MMT layers by two different methods. Similar FT-IR spectra gave further supporting evidence. In order to achieve the pH dependent release of the intercalated PQ molecules, the PQ-MMT complex was

coated with cellulose acetate phthalate (CAP). The ternary system exhibited a strongly suppressed PQ release in the acidic pH domain, while an enhanced PQ release at the neutral pH range.

Three different smectite clays (laponite XLG, saponite, and montmorillonite) intercalated by donepezil were reported by Park et al.³⁰ Powder XRD patterns, TG profiles, and FTIR spectra confirmed that donepezil molecules were well stabilized in the interlayer space of the clays. The thermal stability of the API molecules was also improved after the hybridization. In order to improve dispersibility and formulate a donepezil delivery system with an improved release rate, the hybrids were coated with Eudragit[®] E-100 through spray drying. The release profile of Eudragit[®] E-100 coated hybrid showed a biphasic release pattern, being consisted of a burst and slow release. This suggested that some donepezil molecules encased in clay materials could be replaced by Eudragit[®] E-100 during the coating process.

CHAPTER 3

EXPERIMENTAL

3.1 Materials

3.1.1 Active Pharmaceutical Ingredient

The active pharmaceutical ingredient (API) used in this study is 4, 4'-Diaminodiphenyl Sulfone (Dapsone) purchased from Sigma-Aldrich. Its structural formula is shown in Figure 3.1.

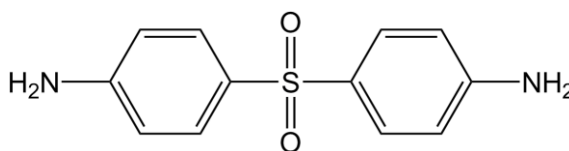


Figure 3.1 Chemical structure of Dapsone.

Dapsone (DAP) is a synthetic derivative of diamino-sulfone with anti-inflammatory and anti-parasitic properties; it has been used to treat leprosy and dermatitis for many years.³¹ It is a yellowish white, odorless crystalline powder with molecular weight of 248.31 g/mol and melting point (T_m) of 175.5 °C.

Because of the two ionizable amino groups, Dapsone has two pK_a values (1.3 and 2.4), and it is expected to be cationic API in its ionized state. Therefore, ionized dapsone could intercalate into the interspacing of a cationic nanoclay through cationic exchange reactions. Dapsone was selected for a miscible API-polymer system since its solubility parameter differs by less than 7.5 MPa^{1/2} from that of the Eudragit[®] S-100 polymer.

3.1.2 Cationic Nanoclay

The cationic nanoclay used in this work is Sodium Montmorillonite (trade name: Cloisite[®]Na⁺, CAS# 1318-93-0) obtained from Southern Clay Products, Inc (Figure 3.2). It is a hydrated aluminum silicate with sodium ions as the predominant exchangeable cation (Cationic Exchange Capacity, CEC = 92.6meq/100g). The chemical formula is $\text{Na}_{0.33}\text{Al}_2\text{Si}_4\text{O}_{10}(\text{OH})_2 \cdot n\text{H}_2\text{O}$, and the basal spacing is 11.7Å.

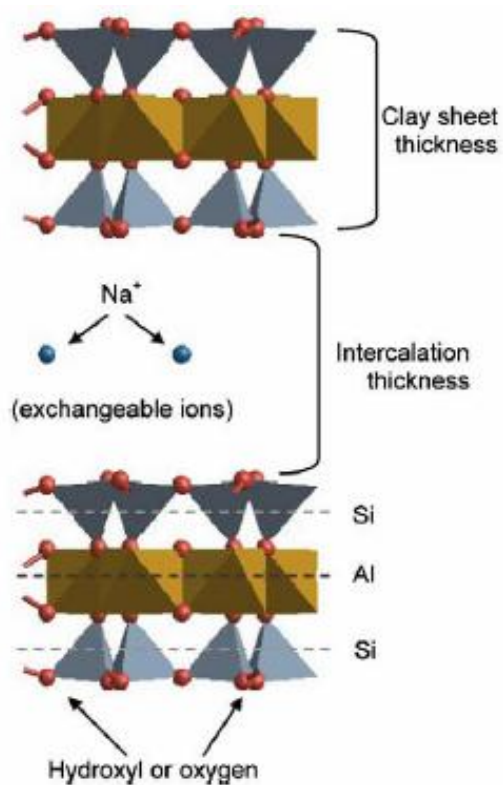


Figure 3.2 Molecular structure of MMT-Na⁺.³²

3.1.3 Polymer Excipient

An amorphous anionic copolymer (Eudragit[®] S-100) based on methacrylic acid and methyl methacrylate (1:2) with pKa value of 6.66 ± 0.05 ³³ donated by Evonik Industries (Piscataway, NJ) (Figure 3.3), was used as the excipient of the API and the API modified clay.

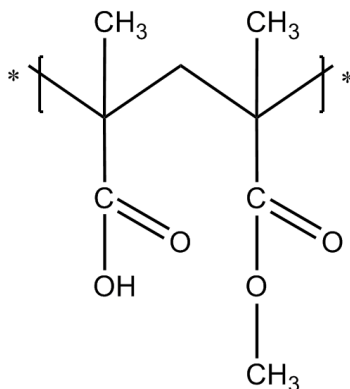


Figure 3.3 Chemical structure of Eudragit[®] S-100.

Eudragit[®] S-100 dissolves in water above pH 7.0, and is expected to be used in ileum and colon targeted delivery. The polymer has a reported T_g of $172\text{ }^\circ\text{C}$ ³⁴ and maximum processing temperature of $186\text{ }^\circ\text{C}$. Considering the narrow range between T_g and processing temperature, a pre-plasticization step was necessary to avoid decomposition of Eudragit[®] S-100 during melt processing. Suitable plasticizers including triethyl citrate, dibutyl sebacate, polyethylene glycol and propylene glycol can reduce the polymer's glass transition temperature and melt viscosity.

3.1.4 Plasticizer

Triethyl citrate (TEC) (Sigma-Aldrich) is a hydrophilic plasticizer used in this study (Figure 3.4). TEC is an oily colorless, odorless liquid with molecular weight 276.3 g/mol and density 1.135 g/cm³. The melting point is -55 °C and boiling point is 294 °C at 101.3 kPa. Triethyl citrate is an environmentally friendly, non-toxic material and its use is permitted as food additive, and in the medical and pharmaceutical fields.

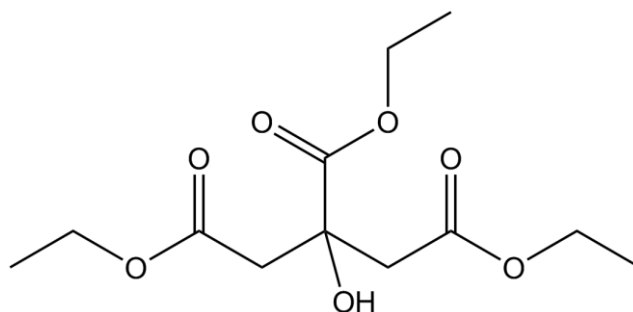


Figure 3.4 Chemical structure of triethyl citrate.

3.2 Sample Preparation

3.2.1 Preparation of Dapsone Functionalized Clay (DAP/Clay)

MMT-Na⁺ (2g) were first dispersed in 200ml distilled water with stirring for eight hours. Dapsone (0.45g, 2x stoichiometric amount based on CEC) was ionized in 10ml 1.0N hydrochloric acid and diluted with 50ml water. Ionized Dapsone solution was added dropwise into the MMT-Na⁺ suspension within one hour. It is to be noted that the initial pH value of 1.7 of the ionized dapsone solution increased to 2.0 after mixing with the clay suspension for one hour. The reacted suspension was then filtered through a Buchner funnel and the cake was washed with distilled water twice to eliminate the excess API. Finally, the products were dried at 60°C for fifteen hours and 80°C for five hours and

ground with mortar and pestle to obtain fine powders. Different experimental conditions were also used and investigated in the intercalation study (Appendix C).

3.2.2 Preparation of Eudragit[®] S-100/DAP, and Eudragit[®] S-100/DAP/Clay Compounds by Melt Mixing

Eudragit[®] S-100 was premixed with 20wt% TEC in a wrist action shaker (Burrell Corporation, Pittsburgh, PA) for 12h. 10wt% DAP, 10wt% DAP modified clay and 10wt% of a DAP/Clay physical mixture were melt compounded with the premix in the batch mixer (PL2000, C. W. Brabender) at 50 rpm and 160°C for 3 minutes. After melt mixing, the samples were pressed into thin disks for further characterization.

3.3 Characterization

3.3.1 Fourier Transform-Infrared (FT-IR) Spectroscopy

FT-IR spectra were obtained on Spectrum One FT-IR Spectrometer[®] (Perkin Elmer Instruments) using the KBr pellet method. Samples (1wt%) were mixed with dry potassium bromide powder and compressed to 13mm discs by a torque wrench. Each disc was scanned 25 times over the mid infrared range wavelength 400-4000 cm⁻¹. The evaluation was carried out with the Spectrum v3.02 program.

3.3.2 Wide Angle X-Ray Diffraction (WXR)

Wide angle X-Ray diffraction analysis was performed using a Philips PW-3040 diffractometer with Cu target and K_α radiation ($\lambda=0.154$ nm) at 45kV/40mA. All specimens were scanned in the 2 θ range from 2°-40° at a rate of 0.003 %/sec. The

interlayer spacings of unmodified and API modified clays were calculated using Bragg's law of diffraction (Equation 3.1):

$$2d = \frac{n\lambda}{\sin \theta} \quad (3.1)$$

Where $n=1$ in this case, λ is the wavelength of the incident X-ray beam in Å, and θ is the angle of incidence in degrees.

3.3.3 Thermogravimetric Analysis (TGA)

Thermogravimetric analysis (TGA) was performed using TGA Q-50 thermogravimetric analyzer (TA Instruments) in a ramp from room temperature to 500 °C. Samples were placed in an open aluminum pan and heated at a rate of 10 °C/min in nitrogen atmosphere (flow rate 40 cm³/min).

3.3.4 Differential Scanning Calorimetry (DSC)

Glass transition temperatures (T_g) and melting temperatures (T_m) were determined by differential scanning calorimetry (DSC Q-100, TA instruments). Each sample was analyzed at heating and cooling rates of 20 °C/min, over a predetermined temperature range under 40 cm³/min nitrogen flow rate.

3.3.5 Scanning Electron Microscopy (SEM)

The fracture surfaces of polymer compounds were examined by Scanning Electron Microscopy (LEO 1530 VP Emission SEM) at 3-5 keV working voltage.

3.3.6 Energy Dispersive X-Ray Analysis (EDX)

To quantitatively analyze the dispersion of API and clay in the polymer matrix, Energy Dispersive X-ray analysis (EDX) (2400 Perkin-Elmer Elemental Mapping) was used. Elemental mappings made it possible to identify major characteristic elements present on the surface and to determine their distribution. The working voltage was 5 kV and mapping time was 300 seconds for all species.

3.3.7 Elemental Analysis

Elemental analysis was performed by the QTI Laboratories, NJ, USA. Perkin-Elmer 2400 Elemental Analyzer was used for determination of carbon, hydrogen, and nitrogen content in the API modified clay. The nitrogen content was then used for calculating the API content in the nanoclay, since the nanoclay does not contain nitrogen.

3.3.8 Dissolution Test and UV-Vis Analysis

Drug dissolution was studied in a Distek dissolution system 2100A with a Distek temperature control system TCS 0200. Eudragit[®] S-100 compounds with API and API/clay hybrid were compressed into 2mm disks having the same holder geometry (circular). The dissolution medium (1L), pH 7.4 phosphate buffer solution simulated the colonic fluid and was maintained at 37 ± 0.5 °C with paddle rotation speed of 100rpm. 5ml samples were withdrawn at predetermined time intervals. After filtration through a 0.45 µm filter, API concentration was analyzed at 295nm by UV-Vis spectrophotometer (Evolution 60, Thermo Scientific). The experiments were repeated three times.

CHAPTER 4

DISCUSSION

4.1 Results on Clay Modified with Dapsone

4.1.1 FTIR Analysis

FTIR spectra of Dapsone, MMT-DAP, and MMT-Na⁺ are shown in Figure 4.1. In the IR spectrum of MMT-Na⁺, the characteristic band at 803 cm⁻¹ indicates the platy structure of montmorillonite.³⁵ The peaks at 3632 cm⁻¹ and 3447 cm⁻¹ are the characteristic stretching vibrations of the O-H bonds in Al-OH and absorbed water in the layers. The peak at 1649 cm⁻¹ is attributed to the O-H bending vibration. The absorption bands at 1045 cm⁻¹ and 917 cm⁻¹ are the Si-O stretching (in-plane) vibration and the Al-Al-OH bending vibration in the octahedral layer respectively.³⁶ The Si-O bending vibration appears at 529 cm⁻¹.

In the spectrum of Dapsone, the strong stretching vibration of the sulfone group O=S=O is at 1108 cm⁻¹ and the bending (out-of-plane) vibration of *p*-disubstituted aromatic ring at 831 cm⁻¹. The peaks at 1598 cm⁻¹ and 3367 cm⁻¹ correspond to the N-H bending vibration and stretching vibration respectively.³⁷ In the spectrum of MMT-DAP hybrid, the characteristic peaks at 529 cm⁻¹, 803 cm⁻¹ and 1045 cm⁻¹ were the same as those of the sodium montmorillonite; the other newly created peaks can be ascribed to surface coated and/or intercalated Dapsone. The absorption band due to the (O=S=O) stretching vibration became weak and shifted to 1112 cm⁻¹ in the hybrid. Similarly, the peaks of N-H and *p*-disubstituted aromatic ring bending vibrations shifted to 1611 cm⁻¹ and 847 cm⁻¹ and both weakened. Compared with the spectra of MMT-Na⁺ and Dapsone, the new absorption band at 3412 cm⁻¹ may be due to the amine group forming chemical

bonds with montmorillonite. The changes taking place in the IR spectrum of the MMT-DAP hybrid indicate that Dapsone is not only attached on the surface but also intercalated in the aluminosilicate layers of montmorillonite.

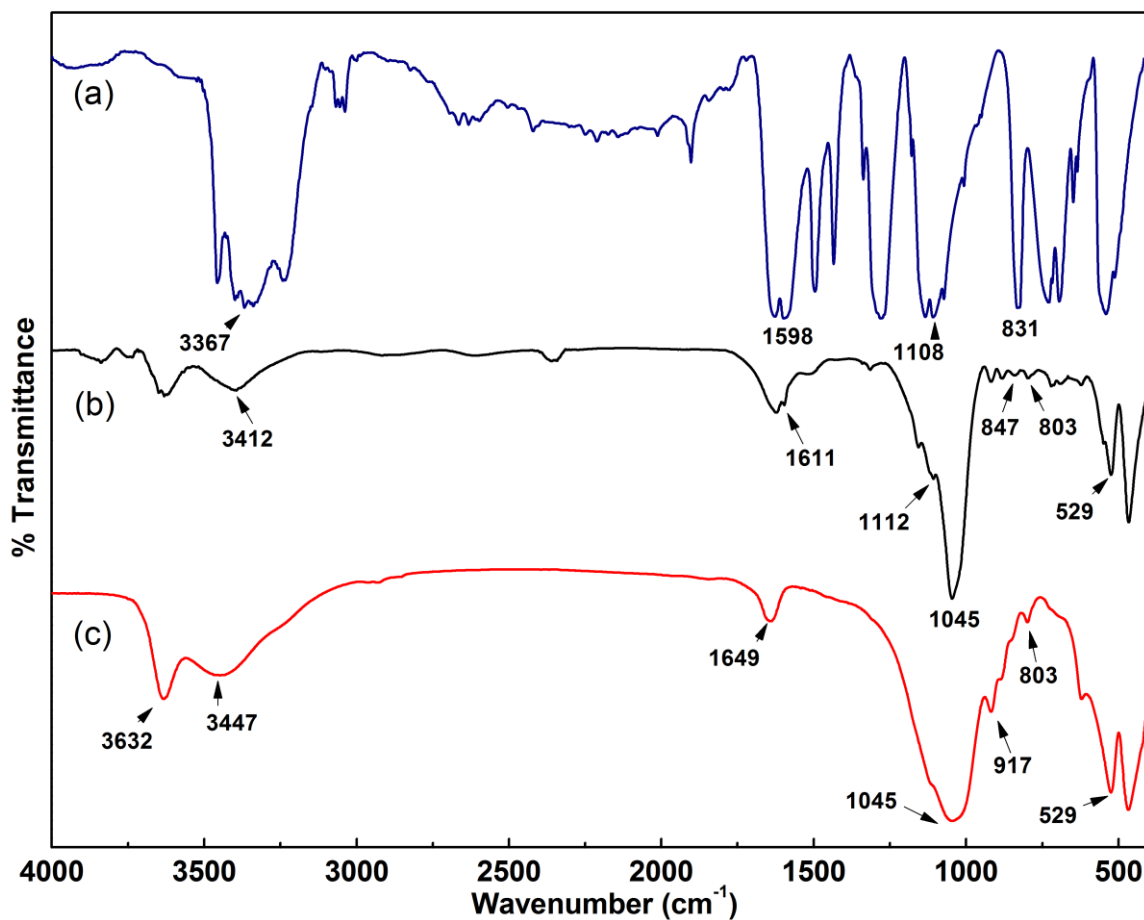


Figure 4.1 FTIR results of (a) Dapsone (DAP), (b) MMT-DAP, and (c) MMT-Na⁺.

4.1.2 XRD Analysis

XRD analysis was used to determine the structural geometry and evaluate the effect of intercalation of Dapsone into the interlayers of montmorillonite. From Figure 4.2, Dapsone appears as a highly crystalline structure containing many sharp peaks. Two

sharp peaks in the MMT- Na^+ XRD pattern are related to the planes (001) and (002) of montmorillonite³⁵. MMT- Na^+ exhibits a strong peak around 7.53° indicating its original basal spacing (d_{001}) is 1.17nm; the peak shifted to 5.69° in the X-ray diffraction profile of the MMT-DAP hybrid corresponding to an increased interlayer spacing (d_{001}) of 1.55nm. This is attributed to the intercalation of Dapsone into the clay interlayer space. The planes (002) of montmorillonite sodium were not affected during the formation of the hybrid.

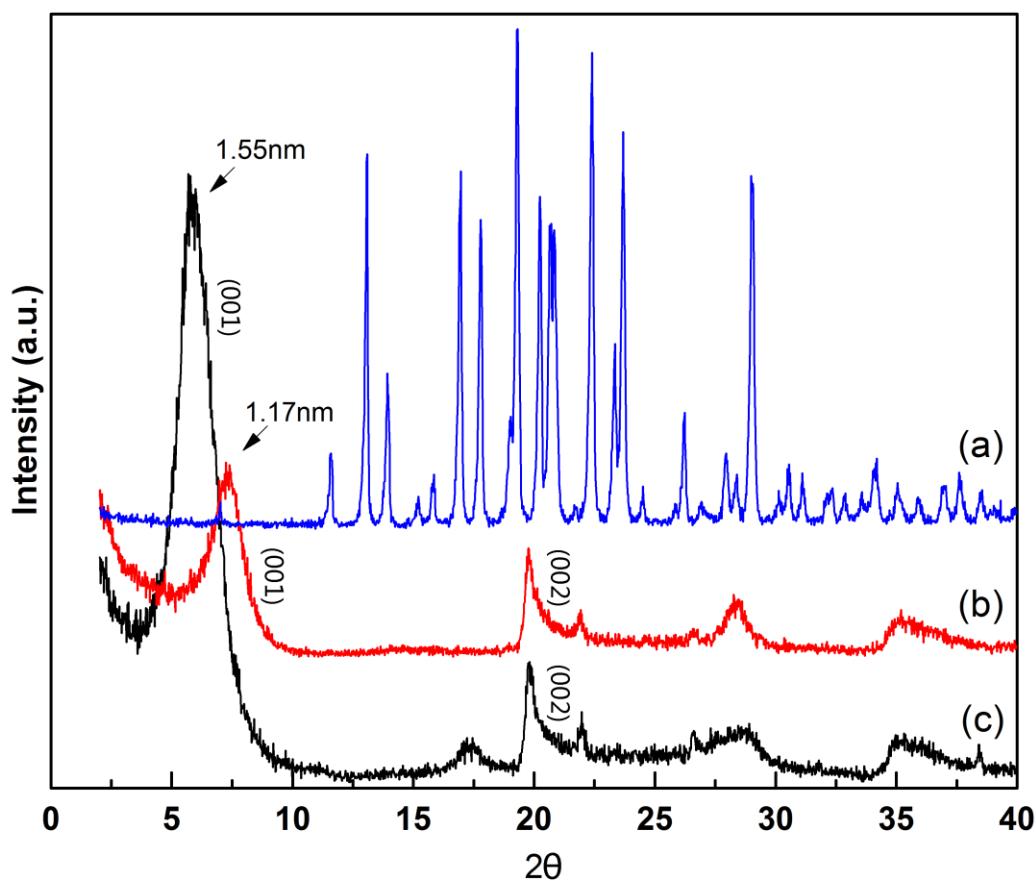


Figure 4.2 XRD results of (a) Dapsone, (b) MMT- Na^+ , and (c) MMT-DAP.

4.1.3 Thermal Analysis

TGA data of MMT- Na^+ , MMT-DAP and Dapsone are shown in Figure 4.3. Dapsone is thermally stable and started decomposing around 300 °C. For MMT- Na^+ and MMT-DAP, the weight loss below 150 °C is attributed to the evaporation of adsorbed water. At higher temperature, MMT- Na^+ does not show weight loss, but MMT-DAP shows a similar pattern of weight loss as compared to the thermal decomposition of Dapsone in the region of 250-500 °C. According to the TGA analysis, after subtracting the moisture content of the MMT-DAP, the approximately 7% additional weight loss could be attributed to the weight of both intercalated and coated Dapsone.

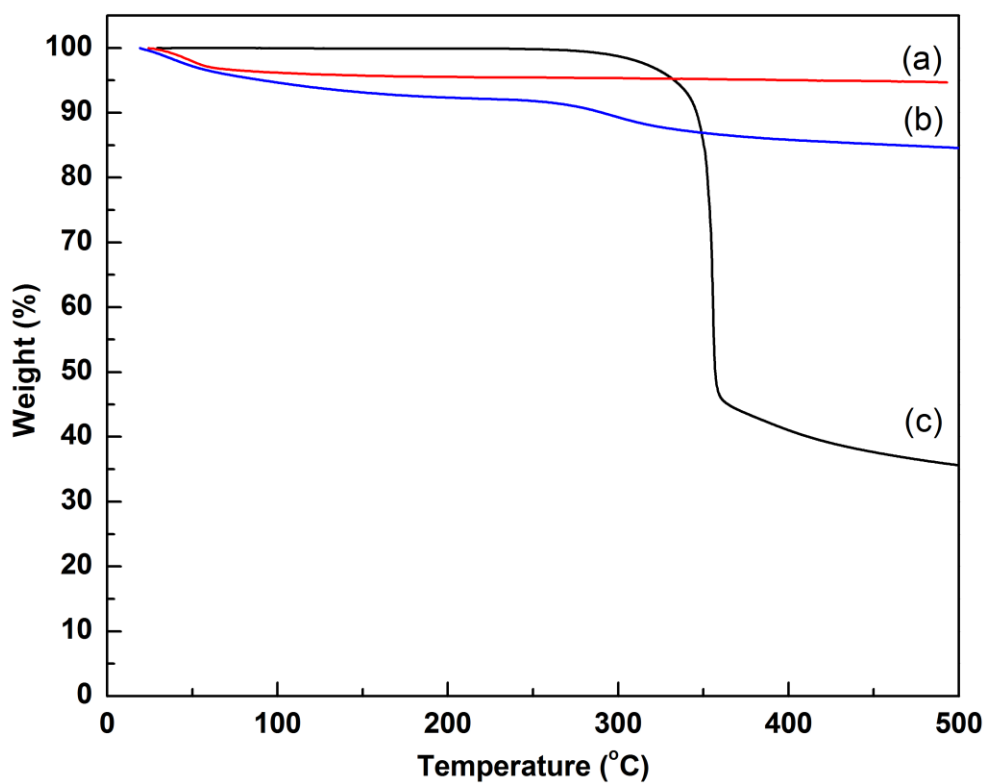


Figure 4.3 TGA results of (a) MMT- Na^+ , (b) MMT-DAP, and (c) Dapsone.

The DSC results (Figure 4.4) show that Dapsone has one strong endothermic peak at 178 °C corresponding to its melting point. MMT- Na^+ does not show any peak, similarly to the MMT-DAP hybrid. This may suggest the presence of intercalated and/or coated Dapsone in an amorphous state.

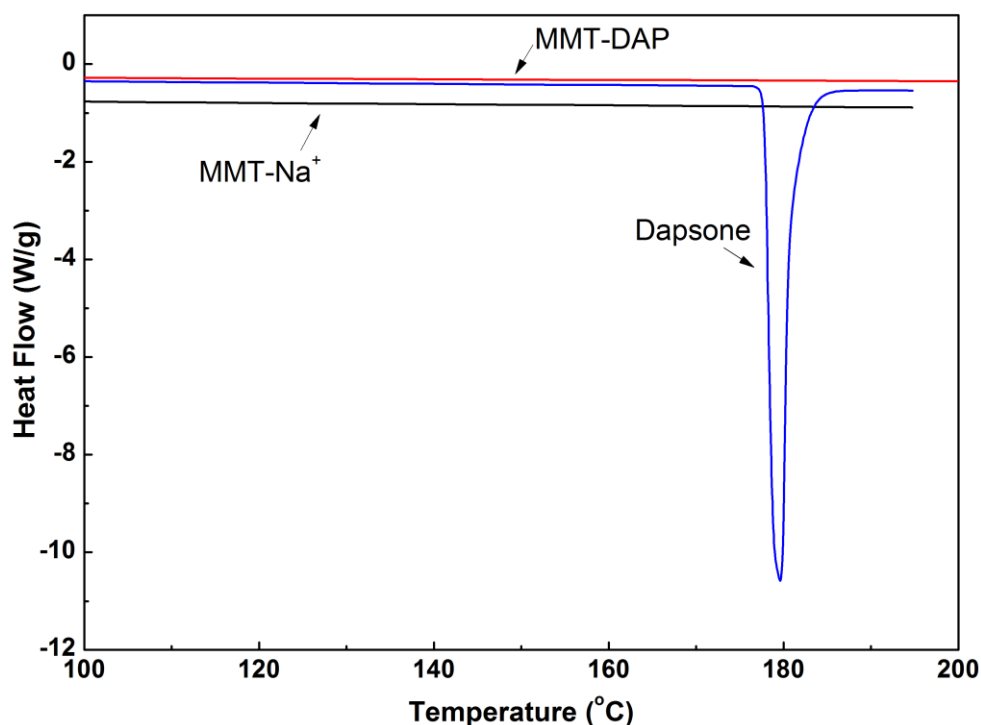


Figure 4.4 DSC results of MMT- Na^+ , MMT-DAP, and Dapsone.

4.1.4 Quantitative Analysis of MMT-DAP

The API loading of MMT-DAP was determined by elemental analysis. Nitrogen is a unique element present only in the API. Therefore, by using this information, the content of Dapsone in the clay can be readily calculated (Appendix A). The calculations based on stoichiometric CEC of MMT- Na^+ indicate that 10.31% Dapsone can be loaded on the clay theoretically; however, from the results of nitrogen elemental analysis, the calculated

Dapsone loading in MMT-DAP is 12.32%. The 2% difference may be due to Dapsone coating the clay surface.

Table 4.1 Results of MMT-DAP Elemental Analysis

Material	% Carbon	% Hydrogen	% Nitrogen
MMT-DAP	7.08	2.05	1.39

4.1.5 Dissolution Test

Figure 4.5 shows the percentage of dissolved API from Dapsone and MMT-DAP as a function of time in a phosphate buffer (pH=7.4). Dapsone shows a slow dissolution profile, by comparison to the much faster dissolution profile in gastric fluid (pH=1.2).

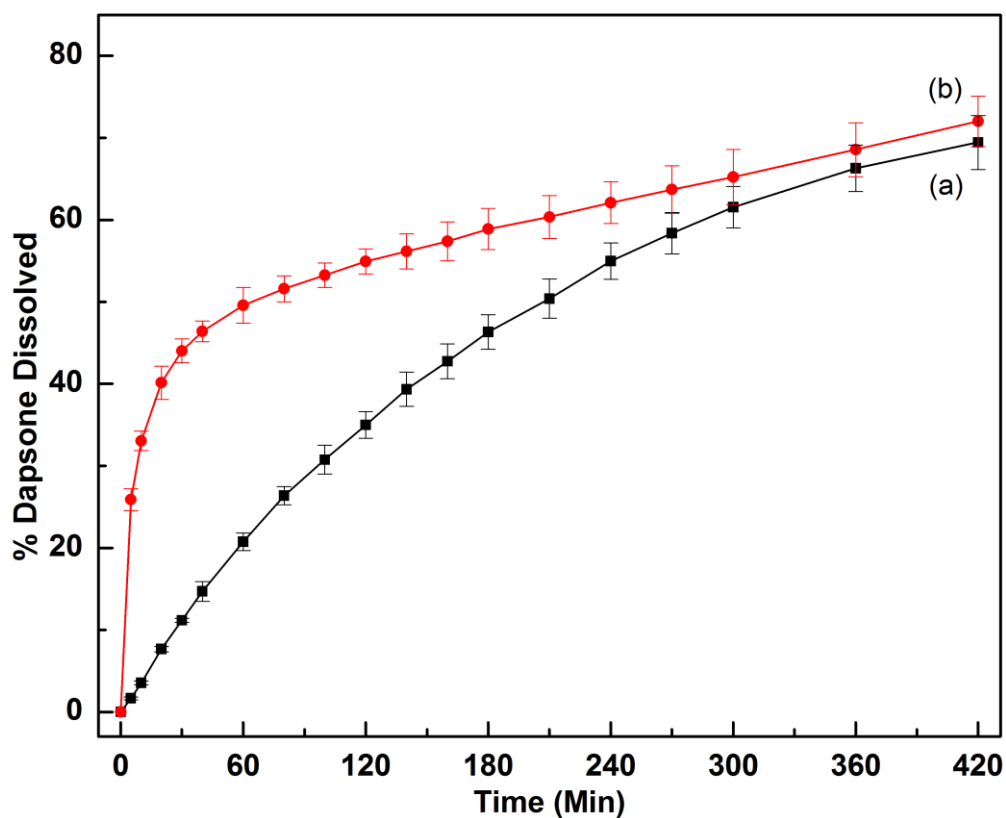


Figure 4.5 Dissolution results in simulated intestinal fluid (phosphate buffer pH=7.4) of (a) Dapsone and (b) MMT-DAP.

MMT-DAP hybrid shows a fast release rate in the first 30 minutes, which is probably due to the rapid release of Dapsone coating the clay surface and its fast dissolution in an ionized form. After 30 minutes, the release rate of Dapsone from MMT-DAP slowed down indicating that the release of the API from the interspacing was dominant. The hybrid also increased the apparent solubility of Dapsone, possibly because the API was present in an ionized and/or amorphous state.

4.2 Results on API Compounded with Eudragit[®]S100

4.2.1 Thermal Analysis

Figure 4.6 shows TGA results of the API, Eudragit[®]S100, plasticizer and blends containing the plasticizer and API. The decreased weight loss of TEC at 130 °C was due to volatilization and possible decomposition. Eudragit[®]S100 without plasticizer had an initial weight loss at 180 °C and began to decompose at 370 °C. The polymer combined with TEC started losing 20wt% at 130 °C. Due to processing difficulties at low temperatures, 160 °C was selected as the compounding temperature; also, the expected evaporation loss could reduce the concentration of TEC in the polymer to a lower value. After hot-melt mixing with the API, the TG analysis indicates the higher API concentration in the polymer matrix could increase the thermal stability of the blend, which could be mainly due to the presence of the more thermally stable Dapsone.

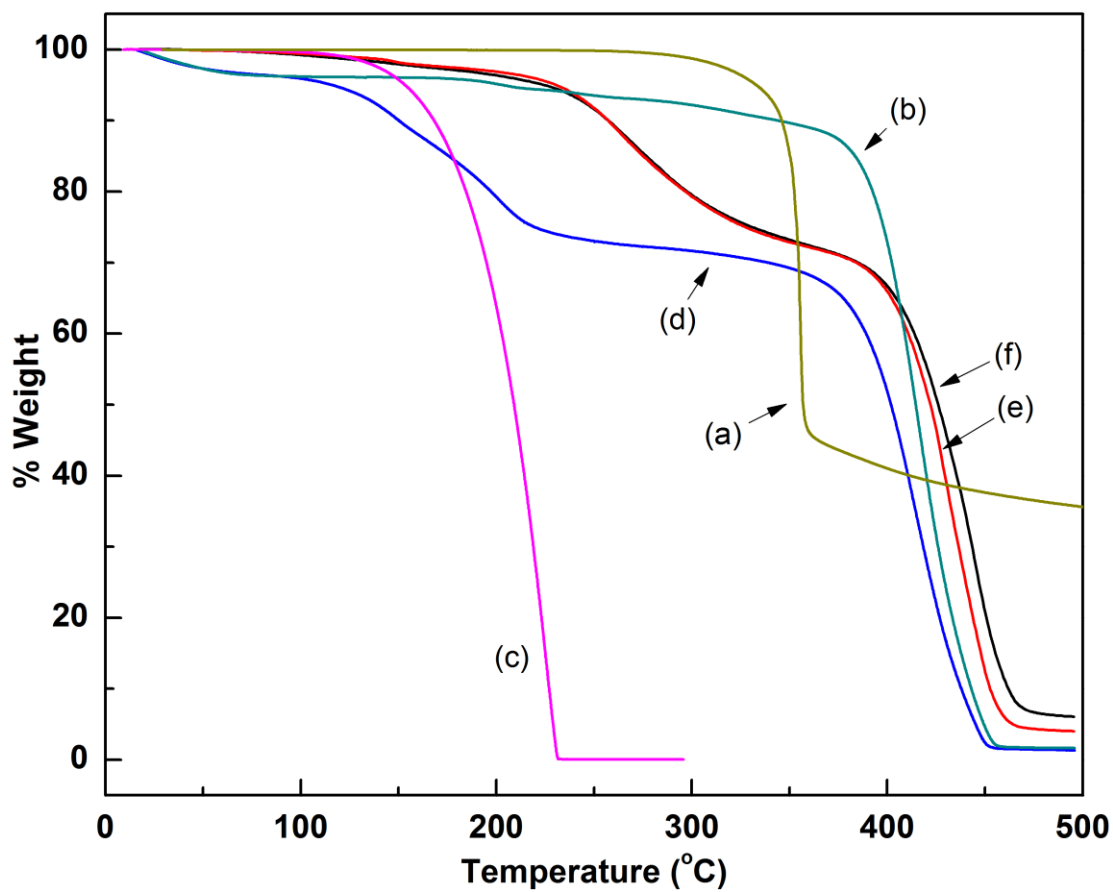


Figure 4.6 TGA results of (a) Dapsone, (b) Eudragit[®]S100, (c) TEC, (d) Eudragit[®]S100/ 20wt% TEC, (e) Eudragit[®]S100/ 20wt% TEC-5wt% DAP, and (f) Eudragit[®]S100/ 20wt% TEC-10wt% DAP.

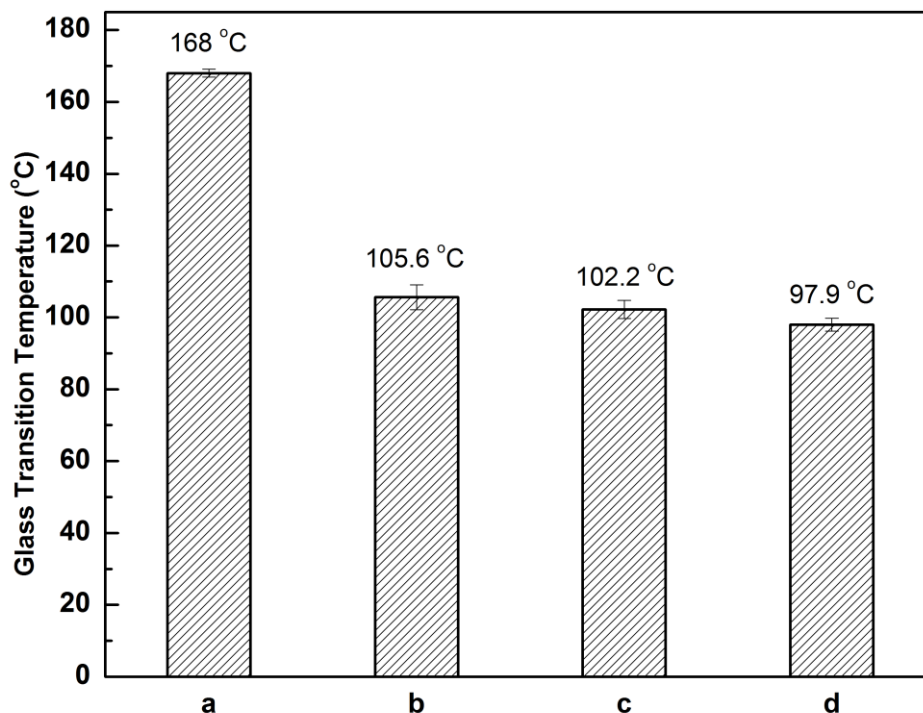


Figure 4.7 T_g of (a) Eudragit®S100, (b) Eudragit®S100/ 20wt% TEC, (c) Eudragit®S100/ 20wt% TEC-5wt% DAP, and (d) Eudragit®S100/ 20wt% TEC-10wt% DAP.

In Figure 4.7, the T_g of the DAP-polymer blends decreased with increasing API loadings. Generally, in amorphous miscible systems, the presence of the smaller API molecules can dilute and weaken the cohesive interactions between the polymer chains. This can enhance the molecular mobility of polymer chains by increasing the free volume in the polymer matrix.²¹

4.2.2 XRD Analysis

Figure 4.8 shows XRD results of Dapsone and Eudragit®S100/DAP composites. As discussed before, the Dapsone spectrum suggests a high degree of crystallinity. When compared with plasticized Eudragit®S100, besides a peak around $2\theta = 13^\circ$, the API-polymer blends do not show other crystalline peaks. The single peak was considered as

an indication of impurity in the Dapsone raw material, which was further confirmed by polarized microscopy. Therefore, it is evident that after hot-melt mixing Dapsone is present in an amorphous state in the polymer matrix.

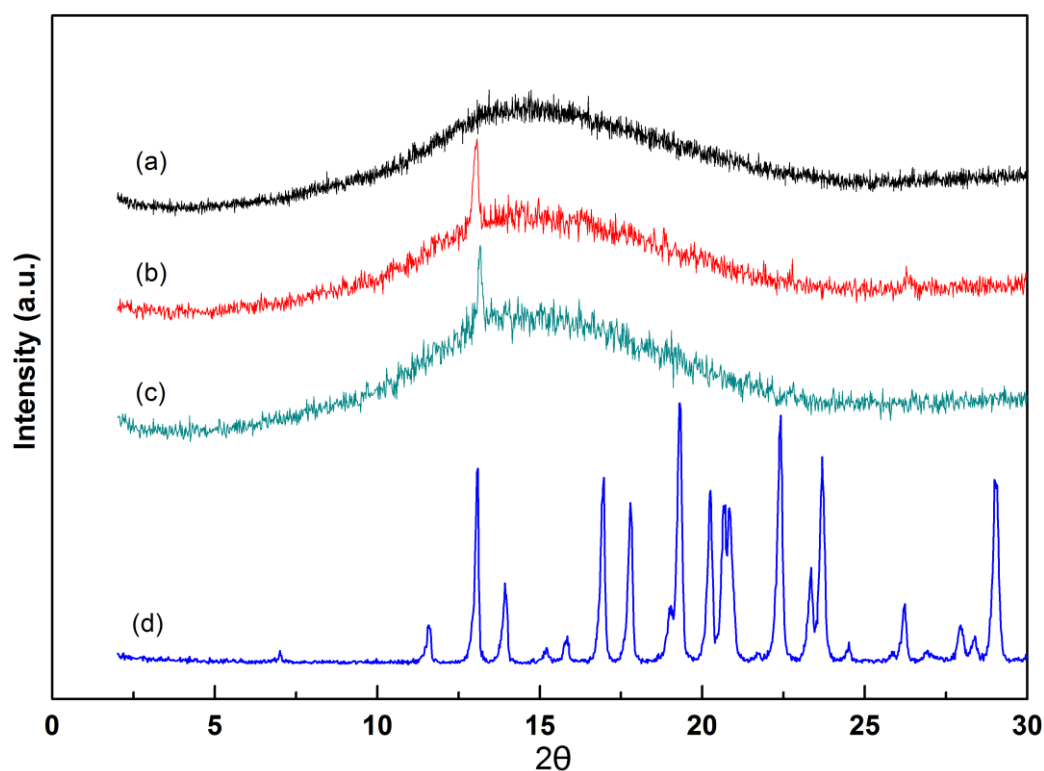


Figure 4.8 XRD results of (a) Eudragit[®]S100/ 20wt% TEC, (b) Eudragit[®]S100/ 20wt% TEC-10wt% DAP, (c) Eudragit[®]S100/ 20wt% TEC-5wt% DAP, and (d) Dapsone.

4.2.3 Morphology

Polarized light microscopy, SEM images and EDX sulfur mapping confirmed the absence of crystalline particles and the uniform distribution of a fully dissolved Dapsone in the polymer matrix.

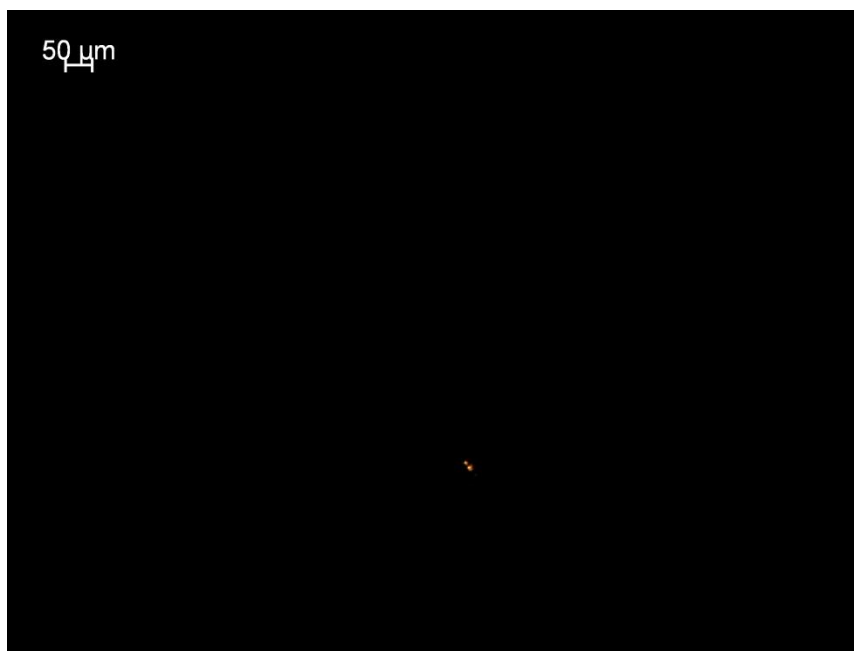


Figure 4.9 Polarized optical microscopy image of Eudragit[®]S100/ 20wt% TEC-10wt% DAP.

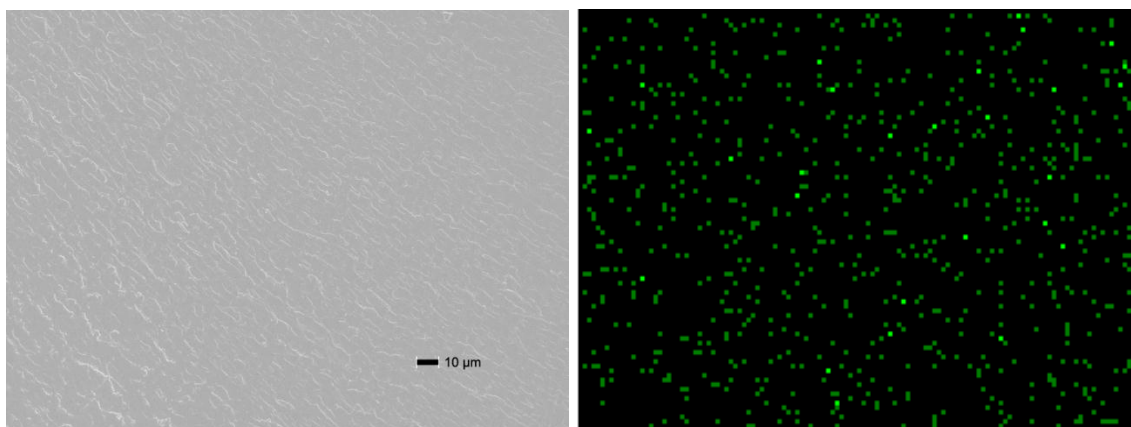


Figure 4.10 SEM image of Eudragit[®]S100/ 20wt% TEC-10wt% DAP (left) and EDX sulfur mapping image of the same region (right).

According to the supplier's specifications, 97% purity Dapsone was used in this study, and by comparing with its X-ray diffraction profile, the particles observed in Figure 4.9 are concluded to be impurities. From the SEM image, the entire surface is

quite smooth and the EDX sulfur mapping (Figure 4.10) further confirms that Dapsone was fully dissolved in the polymer matrix.

4.2.4 Dissolution Test

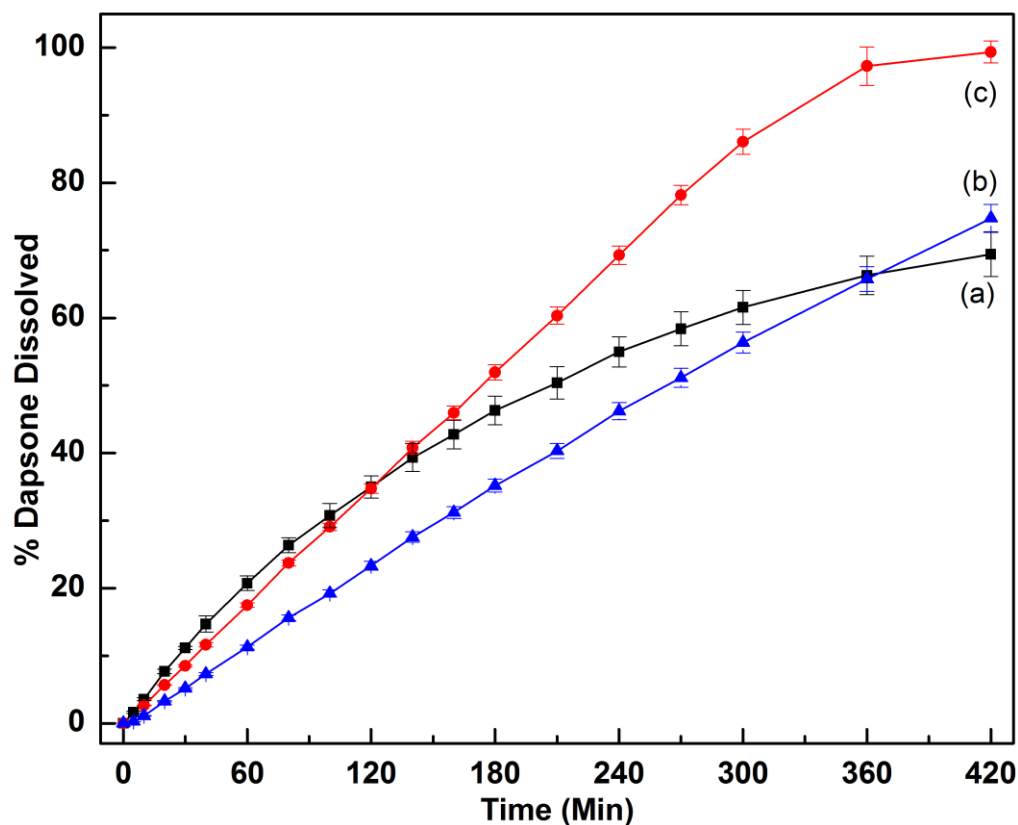


Figure 4.11 Dissolution results in simulated intestinal fluid (phosphate buffer pH=7.4) of (a) Dapsone, (b) Eudragit®S100/ 20wt% TEC-5wt% DAP and (c) Eudragit®S100/ 20wt% TEC-10wt% DAP.

Figure 4.11 shows the dissolution profiles of Dapsone and Eudragit®S100 blends in phosphate buffer solution. The API-polymer blends showed zero-order release profiles, and the release rate increased with increasing API loading. The TEC content in the tablets can increase the API release rate due to the leaching of the water soluble plasticizer during the dissolution test, leading to channel formation in the tablets. Also, during the

dissolution process at pH 7.4, the carboxylic groups in the polymer are ionized and can interact with the amine groups in the Dapsone molecule through ionic bond formation or hydrogen bonding.³⁸ It was hypothesized that following an increase in API loading, the chemical and physical interactions between the functional groups of Eudragit®S100 and Dapsone would also increase, resulting in higher release rate. Needless to mention that the release rate also depends on the size and geometry of the hot-melt processed tablets. In this dissolution test, 25 mm diameter and 2 mm thickness tablets were used and the weight of each sample was 750 ± 30 mg. On the basis of fully dissolved sample (c), after 7 hours, approximately 200 mg of sample (b) containing 5 wt% Dapsone still remained, which further confirms the previous hypothesis. In addition to the favorable interactions between molecules of API and polymer, the API's increased solubility can be explained based on the API's amorphous state in the polymer matrix.

4.3 Results on DAP Modified Clay Compounded with Eudragit[®]S100

4.3.1 Thermal Analysis

Figure 4.12 shows TGA results of Eudragit[®]S100 plasticized with 20 wt% TEC and of the plasticized composites blended with Dapsone, DAP/MMT-Na⁺ physical mixture and MMT-DAP hybrid.

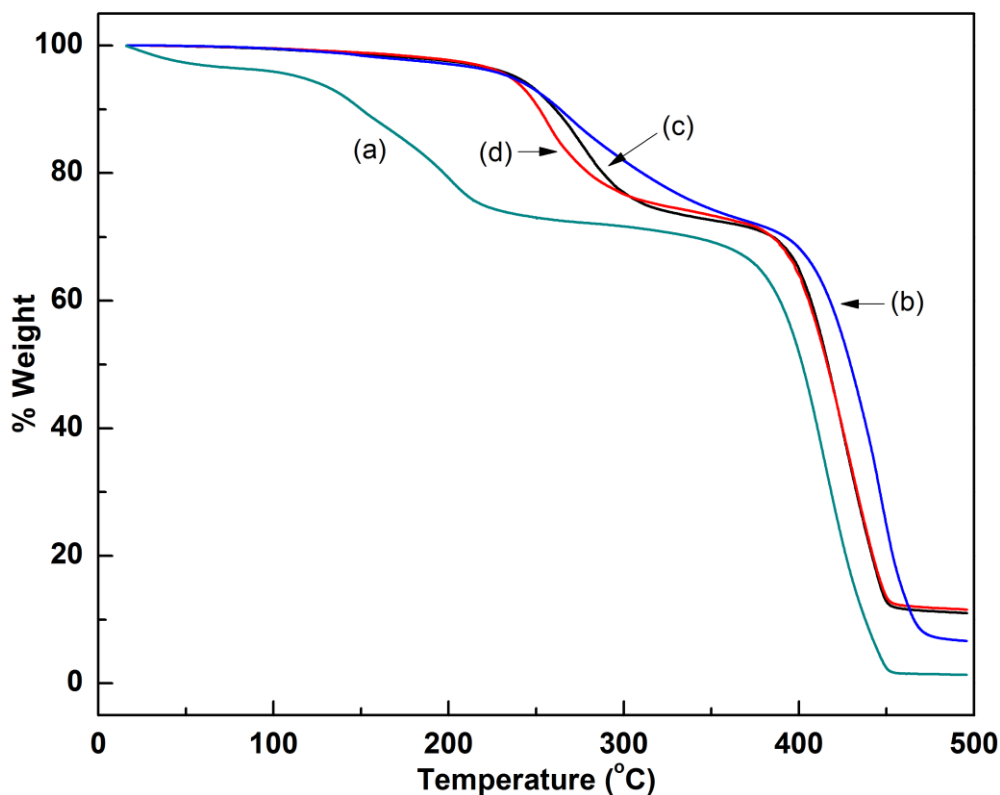


Figure 4.12 TGA results of (a) Eudragit[®]S100/ 20wt% TEC, (b) Eudragit[®]S100/ 20wt% TEC-10wt% DAP, (c) Eudragit[®]S100/ 20wt% TEC-10wt% (DAP/MMT-Na⁺ physical mixture), and (d) Eudragit[®]S100/ 20wt% TEC-10wt% (MMT-DAP hybrid).

In samples (b), (c) and (d), the amount of additives were all 10 wt% based on the amount of plasticized Eudragit[®]S100. Also, for comparison, the amount of Dapsone used in the DAP/MMT-Na⁺ physical mixture was in the same proportion as that in the MMT-DAP hybrid (12.32 wt%). Figure 4.12 indicates that adding the DAP/MMT-Na⁺ physical

mixture and the MMT-DAP hybrid into the plasticized polymer can slightly reduce the thermal stability, which is probably due to the layered structures of montmorillonite that can catalyze the degradation of polymer matrices.³⁹ Compared with the pristine sodium montmorillonite, the average particle size of API modified clay is much larger, which may be the reason of the lower thermal stability.

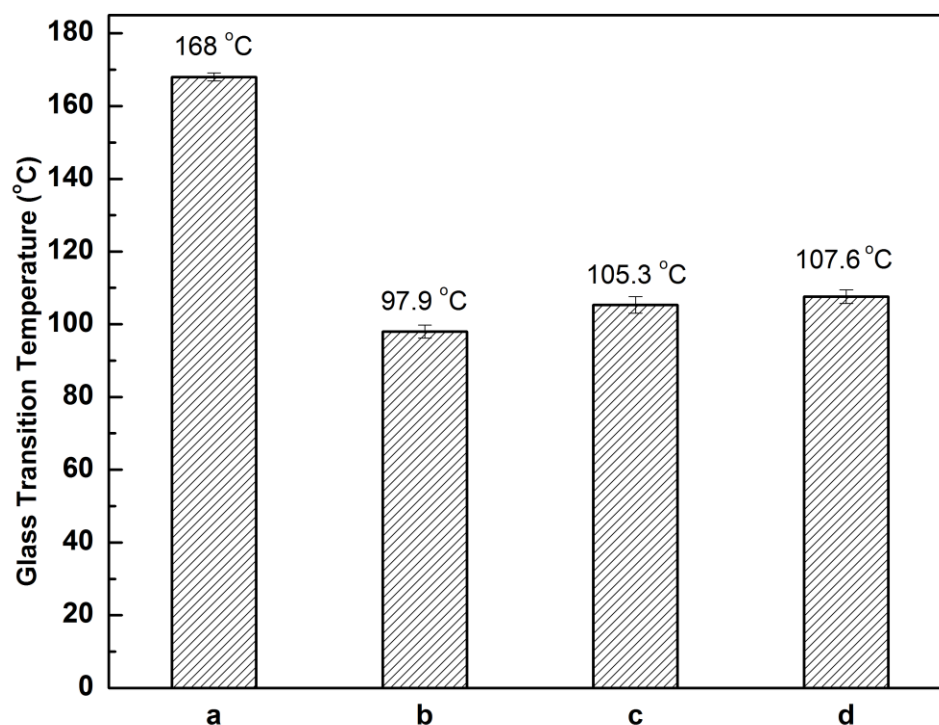


Figure 4.13 T_g of (a) Eudragit[®]S100, (b) Eudragit[®]S100/ 20wt% TEC-10wt% DAP, (c) Eudragit[®]S100/ 20wt% TEC-10wt% (DAP/MMT- Na^+ physical mixture), and (d) Eudragit[®]S100/ 20wt% TEC-10wt% (MMT-DAP hybrid).

Figure 4.13 shows the glass transition temperature values of the corresponding samples. Samples (c) and (d) appear to have higher glass transition temperatures than sample (b) as a result of the presence of the nanoclay that could decrease the free volume of the polymer matrix.

4.3.2 XRD Analysis

Figure 4.14 shows the XRD results of MMT- Na^+ , MMT-DAP, and 20 wt% TEC plasticized Eudragit[®]S100 blended with Dapsone, DAP/MMT- Na^+ physical mixture and MMT-DAP.

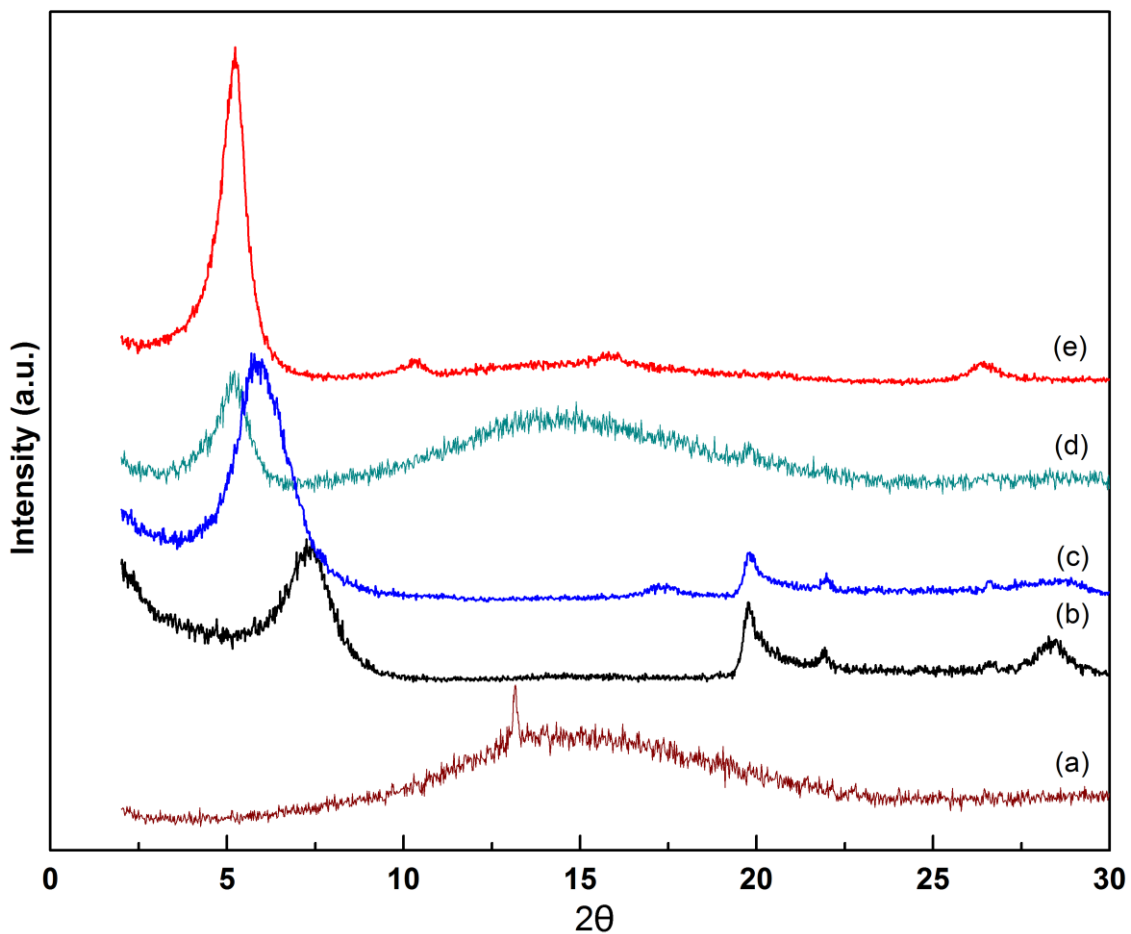


Figure 4.14 XRD results of (a) Eudragit[®]S100/ 20wt% TEC-10wt% DAP, (b) MMT- Na^+ , and (c) MMT-DAP, (d) Eudragit[®]S100/ 20wt% TEC-10wt% (MMT-DAP hybrid), and (e) Eudragit[®]S100/ 20wt% TEC-10wt% (DAP/MMT- Na^+ physical mixture).

Compared with the characteristic peaks of (b) MMT- Na^+ and (c) MMT-DAP, the d_{001} peaks in the profiles of samples (d) and (e) both shifted to a lower angle indicating

that the interspacing of montmorillonite was extended after hot-melt processing. During melt mixing, the polymer chains could penetrate the interlayers of the clay and expanded the spacing. For the XRD profile of sample (d), the weak peak intensity may be due to the presence of Dapsone molecules in the interspacing obstructing the intercalation of polymer chains into the layered structure.

4.3.3 Morphology

Sulfur is one of the unique elements present only in the API and is readily detected by EDX. Figure 4.15 shows a fracture surface of the Eudragit[®] S100 composite containing 20wt% TEC and 10wt% DAP/MMT-Na⁺ physical mixture, and the EDX mappings of elements aluminum, silicon, sodium and sulfur. From EDX analysis, API and clay particles are uniformly dispersed in the Eudragit[®] S100 matrix. One of the areas containing large particles is magnified in Figure 4.16 and Figure 4.17. The layered structures shown in Figure 4.17 indicate the agglomeration of the clay. The images of EDX mapping of aluminum (left) and silicon (right) in Figure 4.16 further confirm the location of montmorillonite agglomerates.

Figure 4.18 shows an SEM image of 10wt% MMT-DAP hybrid in plasticized Eudragit[®] S100 composites, and the corresponding EDX mappings of elements aluminum, silicon and sulfur. By rough approximation from the SEM image, the particles have a wide range of distribution (10 μm - 90 μm) due to the non-uniformity at the grinding step after modification. Sodium was not detected by EDX and the higher population of Al, Si and S overlapped with the larger particles shown in the SEM image, which proved that in combining montmorillonite with Dapsone the sodium was replaced by the API.

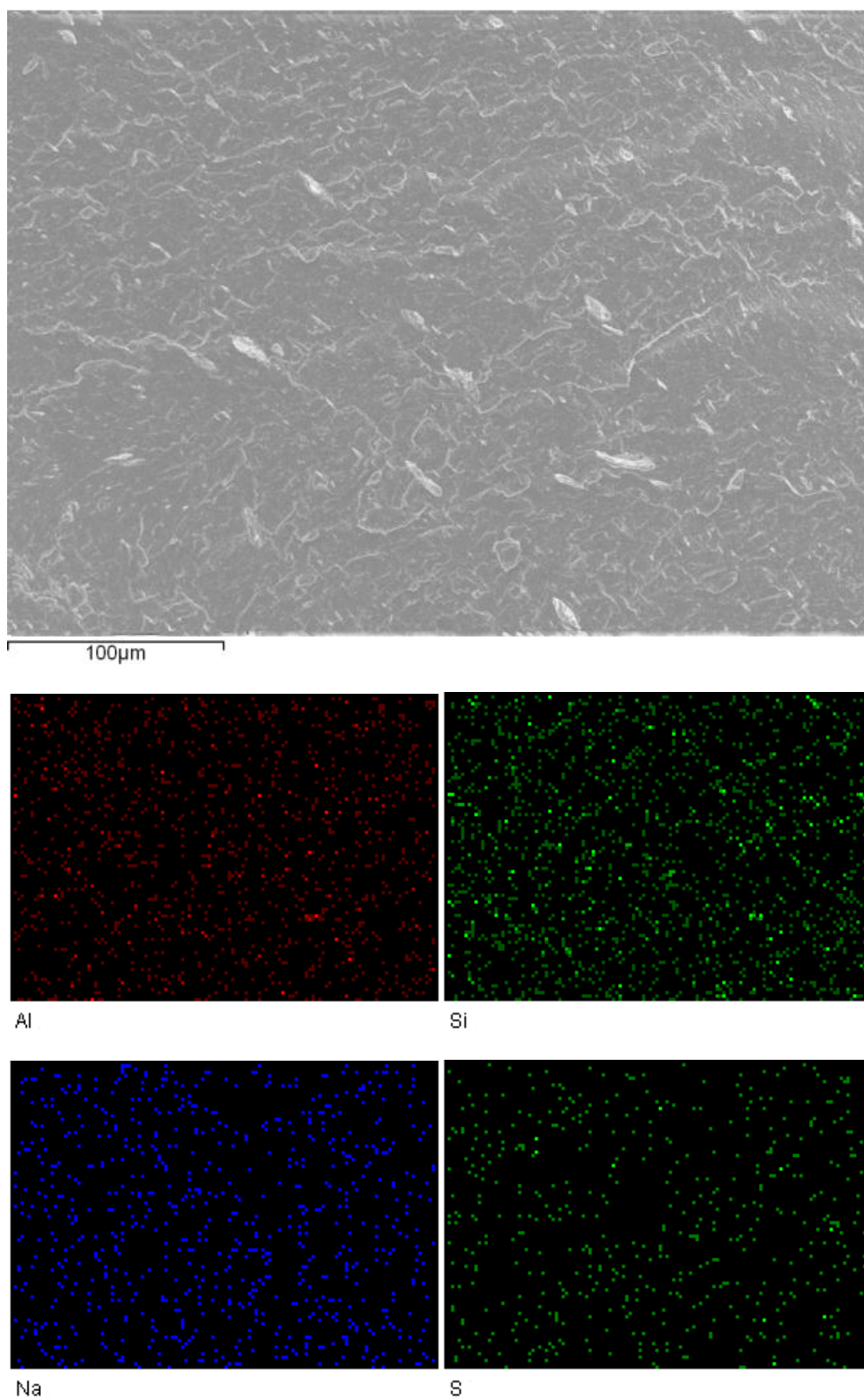


Figure 4.15 SEM image of 10wt% DAP/MMT- Na^+ physical mixture in Eudragit[®]S100 and EDX mappings of elements aluminum, silicon, sodium and sulfur.

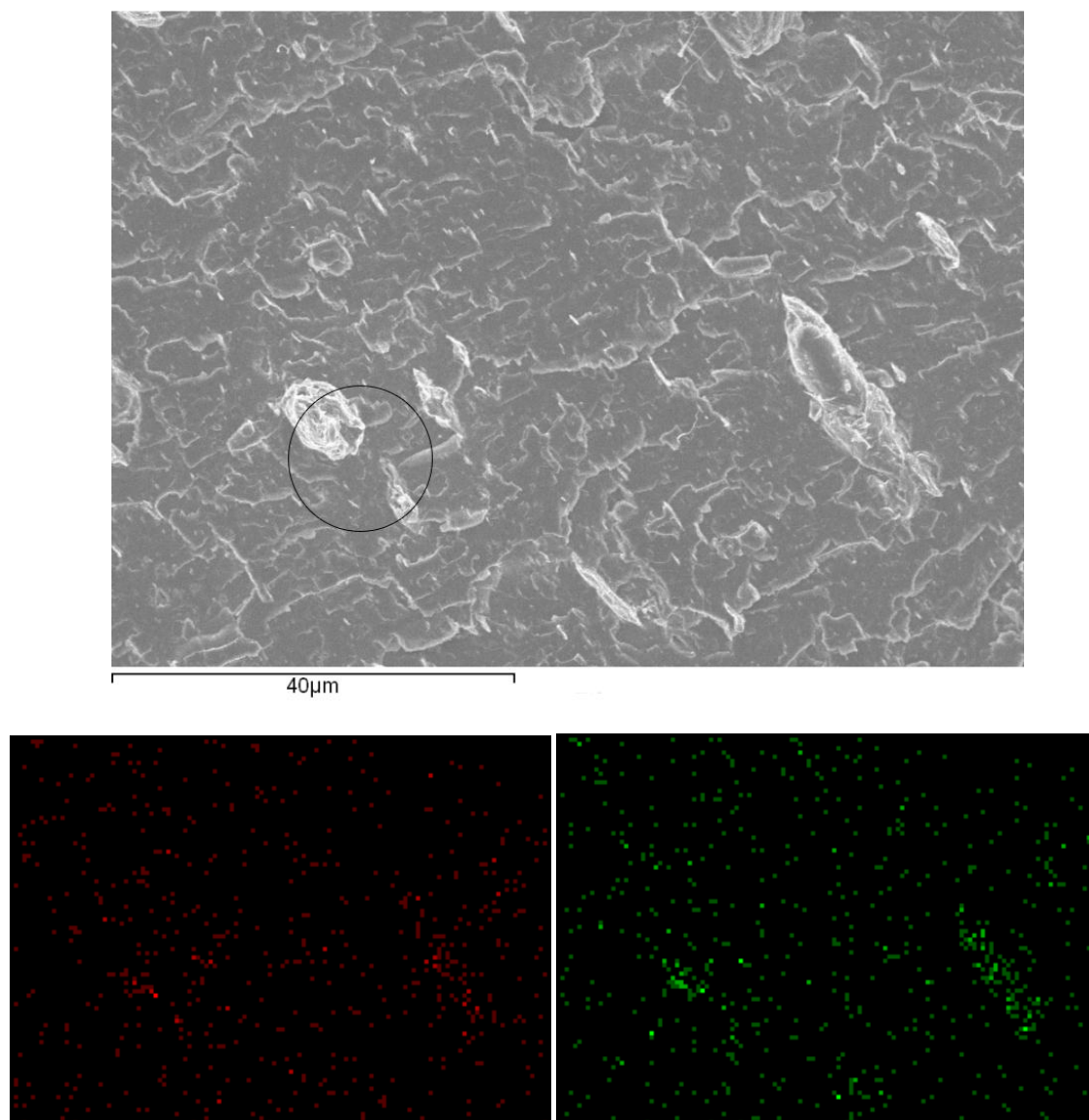


Figure 4.16 SEM image of 10wt% DAP/MMT- Na^+ physical mixture in Eudragit[®] S100 and EXD Mapping of aluminum (left) and silicon (right).

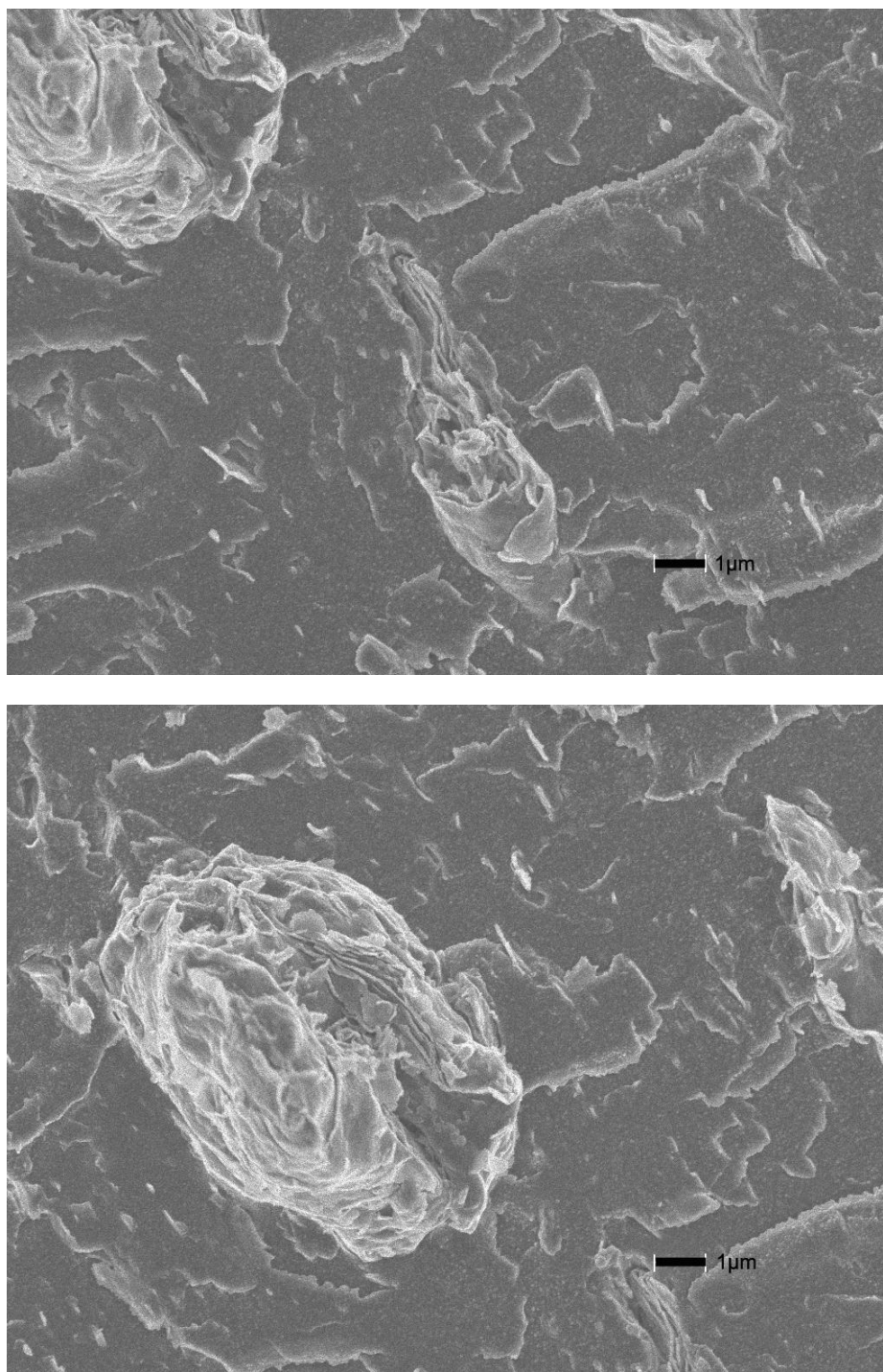


Figure 4.17 Magnified SEM images of the circle shown in Figure 4.16.

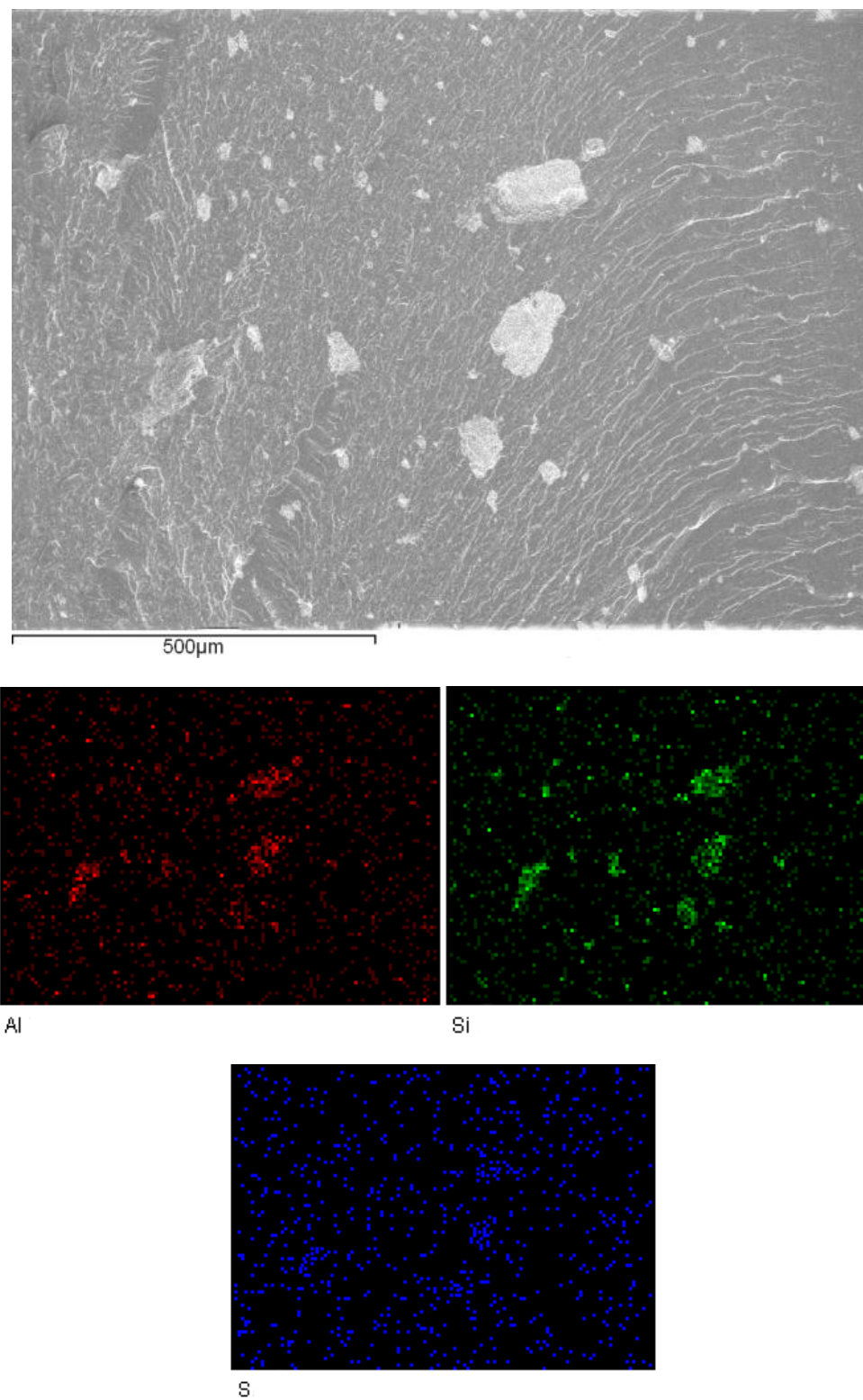


Figure 4.18 SEM image of 10wt% MMT-DAP hybrid in Eudragit[®] S100 and EDX mappings of elements aluminum, silicon and sulfur.

4.3.4 Dissolution Test

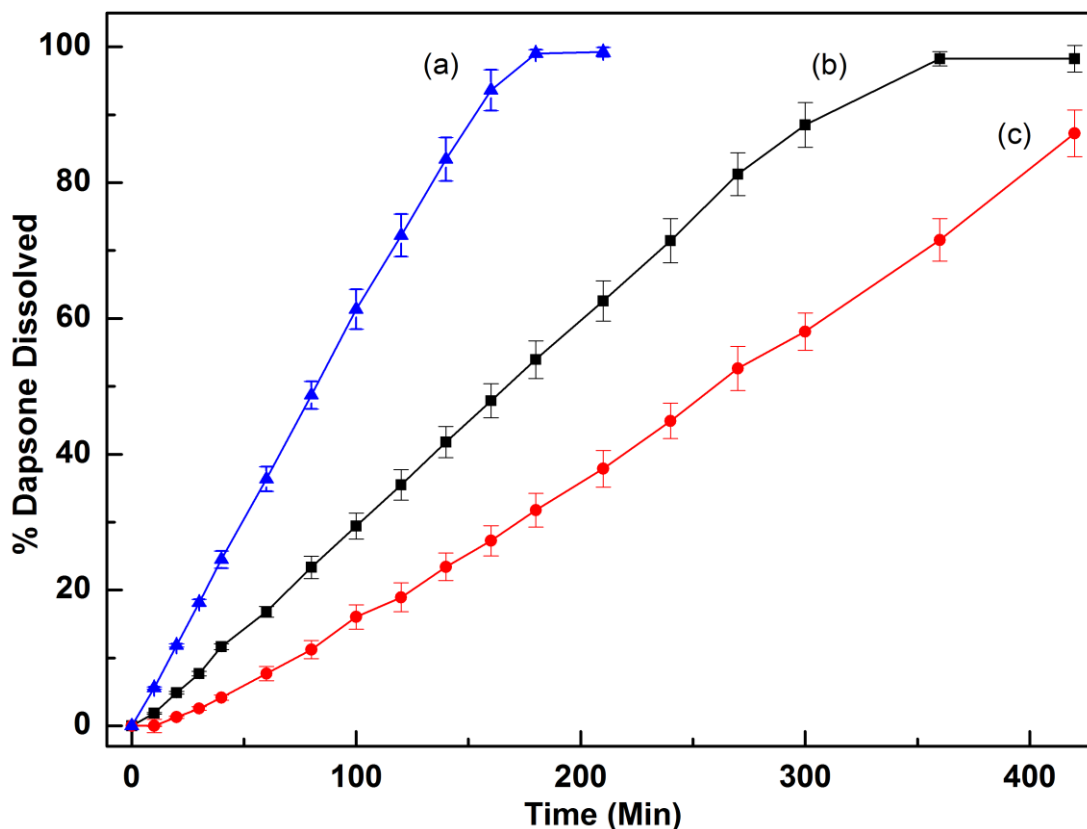


Figure 4.19 Dissolution results in simulated intestinal fluid (phosphate buffer pH=7.4) of (a) Eudragit[®]S100/ 20wt% TEC-10wt% DAP, (b) Eudragit[®]S100/ 20wt% TEC-10wt% (DAP/MMT-Na⁺ physical mixture), and (c) Eudragit[®]S100/ 20wt% TEC-10wt% (MMT-DAP hybrid).

Figure 4.19 shows the dissolution profiles of plasticized Eudragit[®]S100 composites with API, API-clay physical mixture and API-clay hybrid in phosphate buffer solution. As discussed before, size and geometry of the tablets can affect the release rate. In order to dissolve all samples within 7 hours, in this dissolution test 30 mm diameter and 1 mm thickness tablets were used and the weight of each sample was 550 ± 20 mg. The API-clay-polymer blends also show zero-order release profiles, and the release rate decreased by adding clay. The montmorillonite platelets may act as a barrier to block the interaction

between Dapsone and polymer functional groups and slow down the Dapsone release process. The sample containing MMT-DAP hybrid shows the slowest release profile since Dapsone was present in the clay interlayers, and it had to experience one more step in its release path. However, this release behavior cannot achieve 100% dissolution of API since the undissolved Dapsone may have been locked in the clay interspacing.

CHAPTER 5

CONCLUSIONS

A cationic nanoclay, sodium montmorillonite, was successfully intercalated by Dapsone. According to the experiments, the intercalation through ion exchange between ionized Dapsone and MMT- Na^+ is a fast process. This may be attributed to the linear chemical structure of Dapsone which can pass through the interlayers of montmorillonite with a relative ease. Temperature and soaking time did not have a significant effect on the modification indicating that the interaction between the Dapsone molecules and the aluminosilicate layers of montmorillonite is effective and strong. According to the XRD patterns, MMT-DAP showed an increased interlayer spacing by comparing with the results of untreated MMT- Na^+ due to being Dapsone intercalated into the clay interlayer space. By contrast to the pure Dapsone having high crystallinity, the API exists in an amorphous state in the hybrid. Also, the amount of intercalated API depends on the cation exchange capacity of the clay. In simulated intestinal fluid, sustained API release from MMT-DAP can also be an indication of intercalated API, whereas fast release at the initial stage was due to the presence of Dapsone coating on the clay. The delayed release of Dapsone in a second stage indicates that the release of the API from the interspacing was dominant.

In a separate part of this work, Eudragit[®]S100 was melt compounded with Dapsone at 5 wt% and 10 wt% loadings. Consistent with the anticipated miscibility based on calculated solubility parameter differences, a miscible system was obtained with Dapsone present in an amorphous state in the polymer matrix. Compared with the high T_g

of Eudragit[®]S100, the polymer/API blends had lower glass transition temperature and increasing thermal stability with increasing Dapsone loading. The presence of the thermally stable Dapsone can enhance the molecular mobility of polymer chains by increasing the free volume in the polymer matrix. The increased apparent solubility of Dapsone from Eudragit[®]S100/Dapsone blends in pH 7.4 buffer solution was mainly attributed to the favorable interactions between molecules of the API and polymer. The water soluble plasticizer can also result in higher release rate of Dapsone.

API modified clay was melt mixed with Eudragit[®]S100 forming a ternary system. By contrast to the binary polymer/API system, the ternary system has higher glass transition temperature and lower thermal stability, perhaps because of the catalytic effect of montmorillonite on the polymer degradation. Use of this ternary system could decrease the release rate as well as increase the apparent solubility of the API in pH 7.4 buffer solution. The presence of nanoclay in the polymer matrix provided one more tortuous API diffusion path to lower the release rate.

In future studies, it would be of interest to identify the different effects of melt mixing by twin screw extrusion and batch mixer on Eudragit[®]S100/DAP and Eudragit[®]S100/MMT-DAP systems. Furthermore, except Dapsone, other cationic APIs with different chemical structure may affect the rate of the intercalation with montmorillonite and the release rate of APIs from the MMT interlayers. A novel application may be possible by using two API/clay systems with different API release rates mixed with a particular polymer, which is expected to achieve staged release.

APPENDIX A

CALCULATION OF API CONTENT IN NANOCCLAY

According to elemental analysis, MMT-DAP contains 1.39 wt% of nitrogen. Every Dapsone molecule has two nitrogen atoms, and the molecular weight of Dapsone is 248.302g/mol. Based on this information, the content of Dapsone in the clay can be calculated.

Step 1. The percentage of nitrogen in Dapsone is:

$$\text{N\%} = \frac{28.0134 \text{ g/mol}}{248.302 \text{ g/mol}} = 11.282\%$$

Step 2. The content of Dapsone in MMT-DAP is:

$$\text{Dapsone\%} = \frac{1.39\%}{11.282\%} = 12.32\%$$

APPENDIX B

CALCULATION OF SOLUBILITY PARAMETERS

The calculation of solubility parameters using the group contribution method is shown below. In the following Tables the symbols represent:

z = functional group

zU = molar cohesive energy

zV = molar volume

For Dapsone,

Table B.1 Hildebrand Solubility Parameters of Dapsone Groups

GROUP, z	${}^zU/\text{kJ}\cdot\text{mol}^{-1}$	$\sum {}^zU/\text{kJ}\cdot\text{mol}^{-1}$	${}^zV/\text{cm}^3\cdot\text{mol}^{-1}$	$\sum {}^zV/\text{cm}^3\cdot\text{mol}^{-1}$
2 Phenylene	31.94	63.88	52.4	104.8
2 (-NH ₂)	12.56	25.12	19.2	38.4
1 (-SO ₂ -) ⁴⁰	39.12	39.12	23.6	23.6
	Total	128.12	Total	166.8

$$\delta = \left(\frac{\sum \Delta e_i}{\sum v_i} \right)^{0.5} = (128120/166.8)^{0.5} = 27.7\text{MPa}^{1/2}$$

For Eudragit[®] S100,

Table B.2 Hildebrand Solubility Parameters of Eudragit[®] S100 Groups

GROUP, z	${}^zU/\text{kJ}\cdot\text{mol}^{-1}$	$\sum {}^zU/\text{kJ}\cdot\text{mol}^{-1}$	${}^zV/\text{cm}^3\cdot\text{mol}^{-1}$	$\sum {}^zV/\text{cm}^3\cdot\text{mol}^{-1}$
3 (-CH ₃)	4.71	14.13	33.5	100.5
1 (-COO-)	18.0	18.0	18.0	18.0
3 (-CH ₂)	4.94	14.82	16.1	48.3
2 (C)	1.47	2.94	-19.2	-38.4
1 (-COOH)	27.63	27.63	28.5	28.5
	Total	77.52	Total	156.9

$$\delta = \left(\frac{\sum \Delta e_i}{\sum v_i} \right)^{0.5} = (77520/156.9)^{0.5} = 22.2\text{MPa}^{1/2}$$

Compounds with similar values of solubility parameters are likely to be miscible. This is because the energy of mixing within the components is balanced by the energy released by interaction between the components²¹. Greenhalgh demonstrated that compounds with $\Delta\delta < 7.0\text{MPa}^{1/2}$ are likely to be miscible while compounds with $\Delta\delta > 10.0\text{MPa}^{1/2}$ are likely to be immiscible.²²

Following these guidelines, since the value for δ of Dapsone is calculated to be $27.7\text{MPa}^{1/2}$ and compared with the values for δ of Eudragit[®] S100, it can be predicted that Eudragit[®] S100 with δ of $22.2\text{MPa}^{1/2}$ is likely to be miscible with the API. The prediction was in agreement with the experimental results where Dapsone particles were dispersed in an amorphous form in Eudragit[®] S100 after hot-melt mixing.

APPENDIX C

INTERCALATION STUDY

In order to achieve maximum intercalation of API into the interlayer of montmorillonite, different experimental conditions were used. Effect of ionization of Dapsone, soaking time, temperature and initial concentration of Dapsone were investigated.

The abbreviations of Dapsone modified MMT-Na⁺ obtained under different cationic exchange conditions are shown in Table C.1.

Table C.1 Abbreviations of MMT-Na⁺ Samples Modified with Dapsone

Abbreviations	Exchange Temperature	Soaking Time	Ionization	API used amount based on CEC
(a) 2xRT24h-N	RT	24h	–	2x
(b) 2xRT24h	RT	24h	√	2x
(c) 2xRT15h	RT	15h	√	2x
(d) 2xRT3h	RT	3h	√	2x
(e) 2xRT1h	RT	1h	√	2x
(f) 2x60°C3h	60 °C	3h	√	2x
(g) 2x60°C1h	60°C	1h	√	2x
(h) 1xRT1h	RT	1h	√	1x

Effect of ionization of Dapsone

Considering that Dapsone is insoluble in neutral pH but its solubility increases in acidic pH and it can dissolve in an organic solvent, two methods were used to identify the effect of the medium of intercalation. The first method (sample (a)) is to dissolve Dapsone in ethanol before clay modification, and the second method (sample (b)) is first to ionize Dapsone with hydrochloric acid. Other ion exchange conditions are kept the same, i.e.,

soaking time 24 hours with continuous stirring at room temperature, twice the stoichiometric amount of API based on the CEC of the clay.

In the XRD analysis shown in Figure C.1, compared with the XRD profile of pristine MMT- Na^+ , a peak at 2θ of 5.69° for sample (b) corresponds to an increased interspacing of 1.55nm and intercalation of Dapsone into the clay interlayer space. By contrast, a peak at 2θ of 8.77° for sample (a) shows that the interspacing shrunk to 1.07nm, an indication that ion exchange did not happen. The shrinkage of interspacing may be attributed to the removed sodium ion in the MMT layers caused by the long soaking time.

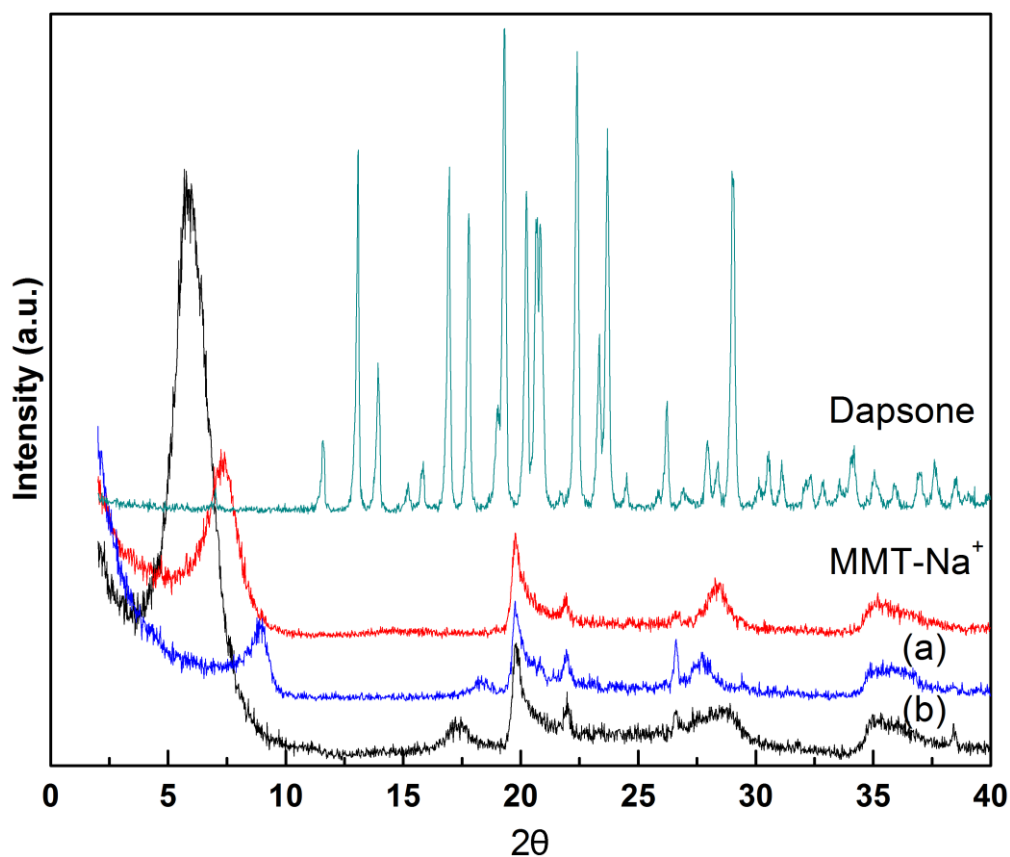


Figure C.1 XRD results of Dapsone, MMT- Na^+ , (a) 2xRT24h-N and (b) 2xRT24h.

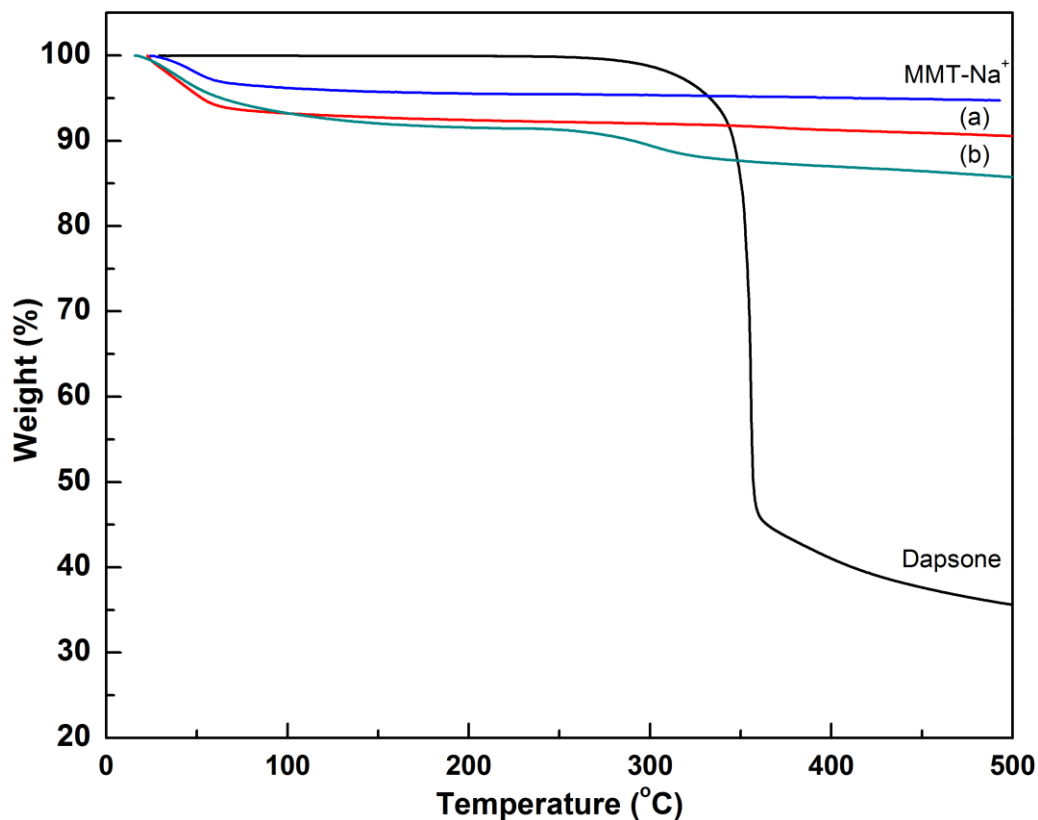


Figure C.2 TGA results of Dapsone, MMT-Na⁺, (a) 2xRT24h-N and (b) 2xRT24h.

The TGA results further indicate that un-ionized Dapsone is not present in the hybrid. In Figure C.2, in the temperature range of 250 °C to 500 °C, the expected weight loss not appears in sample (a). According to sample (b), the weight loss after 250 °C can be ascribed to the Dapsone loaded in the clay. These results suggest that ionization of Dapsone for the ion exchange reaction is necessary.

Effect of soaking time on the intercalation

Ionized Dapsone solution (2x stoichiometric amount based on CEC) was added into 200ml of well dispersed MMT (2g) suspension with continuous stirring at room temperature for 1h, 3h, 15h, and 24h, respectively.

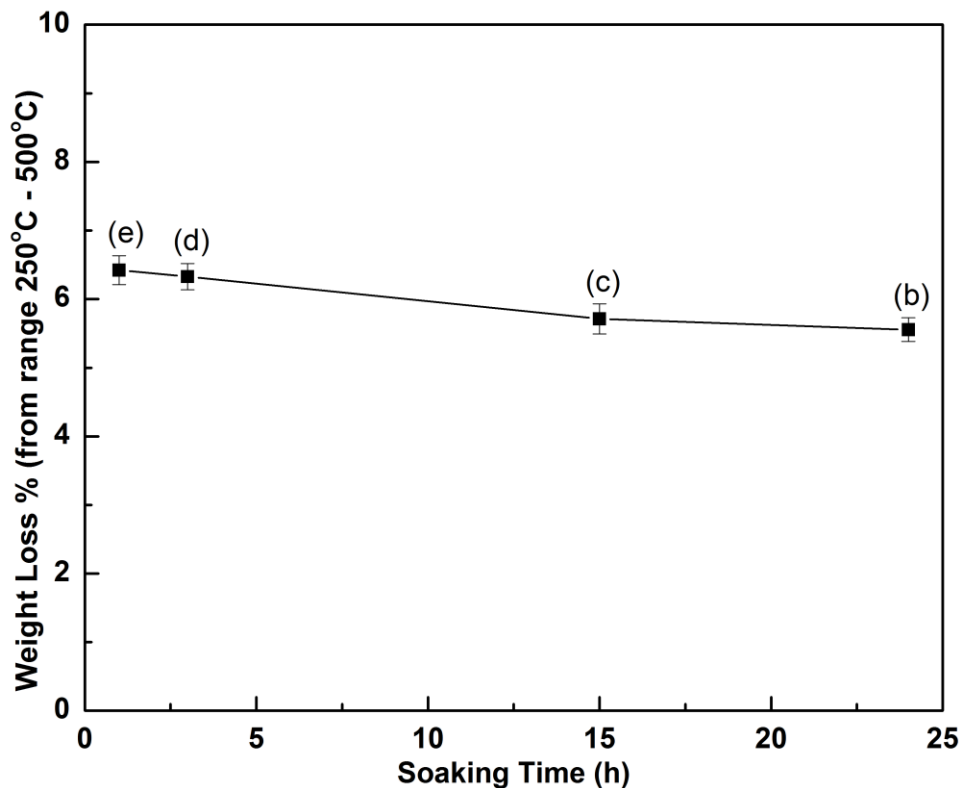


Figure C.3 Weight loss of MMT-DAP hybrids soaked in different times.

The weight loss of API was calculated from TGA results (range 250 °C to 500 °C). Figures C.3 and C.4 show that the intercalation of ionized Dapsone in MMT- Na^+ is a fast process and the soaking time effect on intercalation is negligible. However, it appears that intercalation decreased with increasing soaking time. The major mechanisms of Dapsone intercalation into montmorillonite are: (1) ionized Dapsone adsorbs onto the surface of MMT- Na^+ ; (2) ionized Dapsone replaces sodium ions and is present in the basal spacing of the clay. The very rapid intercalation may be attributed to the linear chemical structure of Dapsone which can then pass through interlayers of montmorillonite with relative ease. Followed the time increasing, the intercalated Dapsone could pass through the interspacing and re-coated onto the clay surface. After washing and filtering, the surface Dapsone can be washed away, thus resulting in a

decrease of API loading. Also, since montmorillonite is unstable in very acidic conditions interaction time was set to 1 hour and the Dapsone solution was added dropwise into the clay suspension.

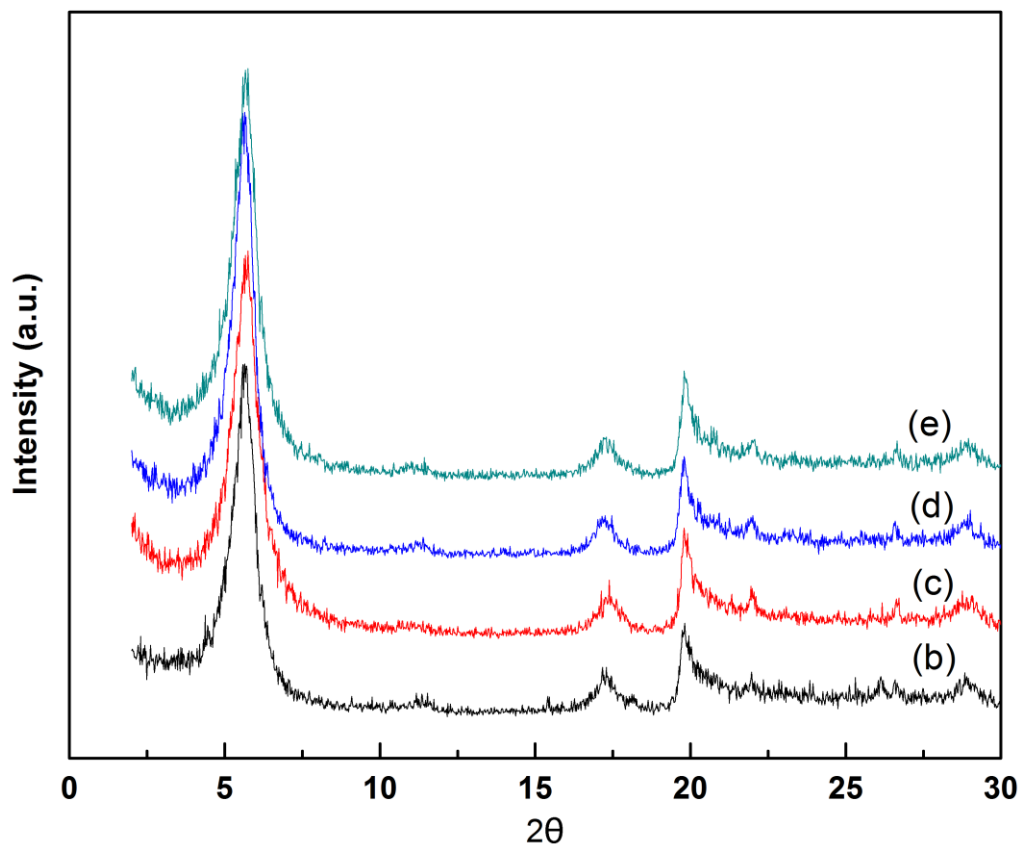


Figure C.4 XRD results of (b) 2xRT24h, (c) 2xRT15h, (d) 2xRT3h and (e) 2xRT1h.

Effect of temperature on intercalation

To study the effect of temperature in short soaking time, two groups of samples were used. Group one contains sample (e) and sample (g) reacted for 1 h at room temperature and 60 °C, respectively. The second group contains sample (d) and sample (f) reacted for 3 h at room temperature and 60 °C, respectively. The trends in Figure C.5 indicate that in short intercalation times, higher temperature could decrease the API loading. High temperature can affect rapid molecular motion of Dapsone during ion exchange leading

to easier penetration of Dapsone molecules through clay interlayers, in which the API ions are supposed to attach but finally will be filtered or washed away. However, the temperature effect on intercalation is also not obvious. Figure C.6 shows the XRD data of those four samples indicating that intercalation to different degrees took place in each sample.

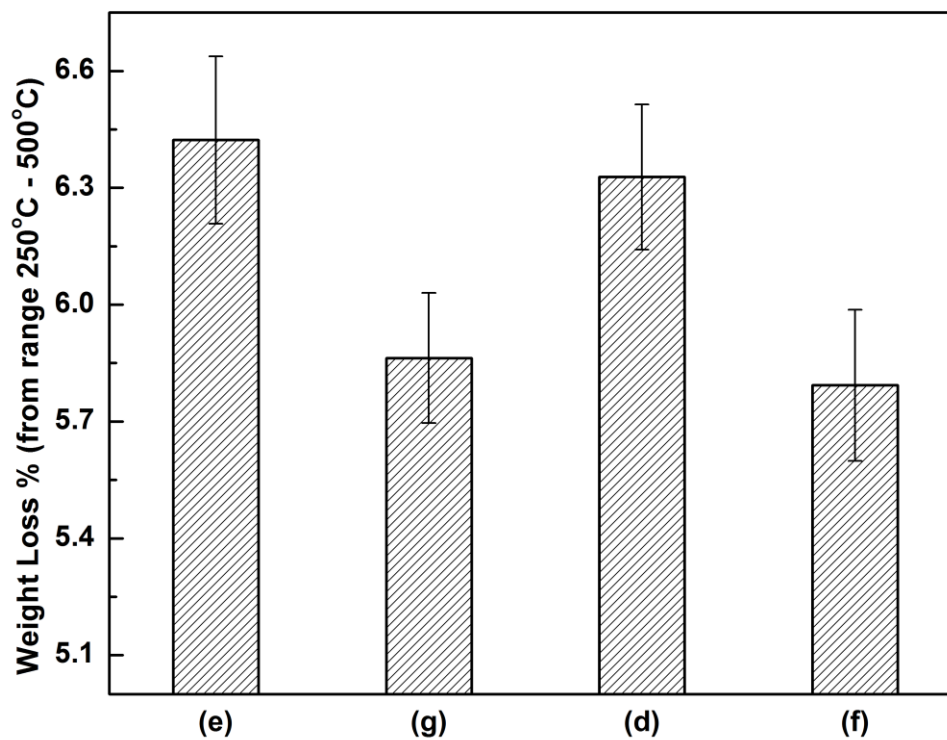


Figure C.5 Intercalation of Dapsone at different temperatures.

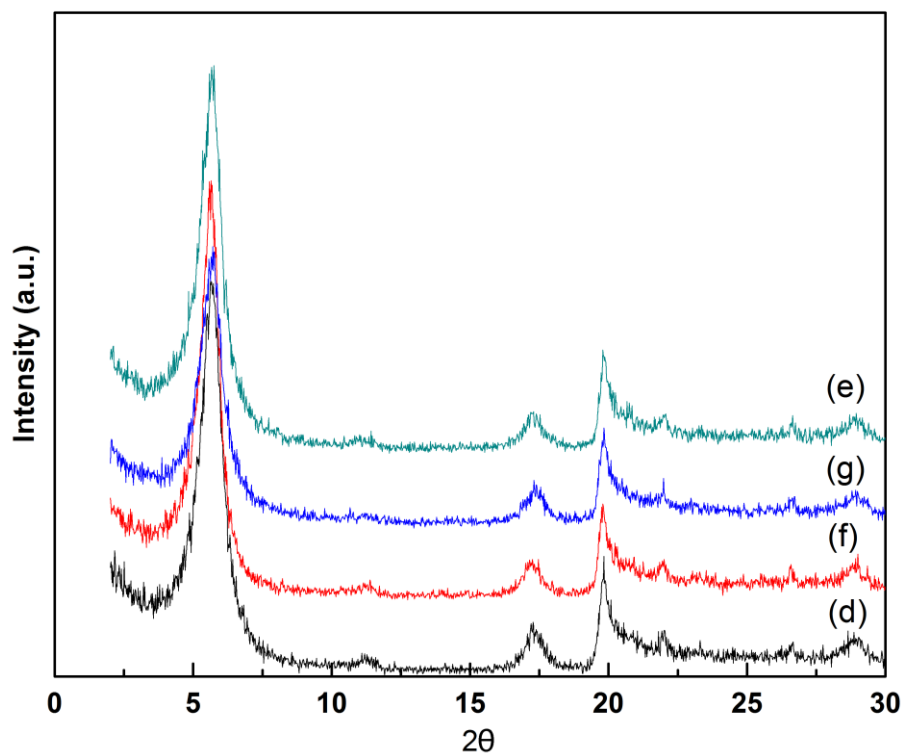


Figure C.6 XRD results of (d) 2xRT3h, (e) 2xRT1h, (f) 2x60°C3h and (g) 2x60°C1h.

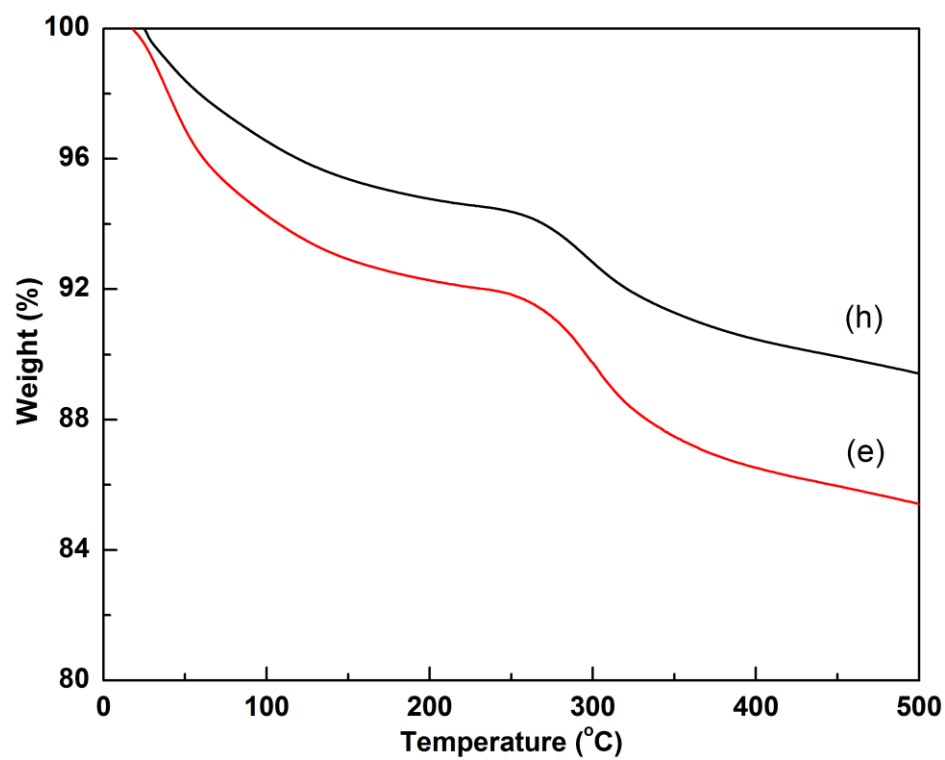


Figure C.7 TGA results of (e) 2xRT1h and (h) 1xRT1h.

Effect of initial Dapsone concentration on intercalation

Based on the cation exchange capacity of montmorillonite, stoichiometric and twice the stoichiometric amounts of Dapsone were used. From Figure C.7, the TGA result shows that in one hour intercalation time, the API loading of sample (h) is less than the API loading of sample (e). Therefore, twice the stoichiometric amount of Dapsone is needed to eliminate incomplete intercalation.

REFERENCES

1. Waterbeemd, D. H. v. d.; Testa, P. D. B., Introduction: The Why and How of Drug Bioavailability Research. In *Drug Bioavailability (Second Edition)*, Dr. Han van de Waterbeemd, P. D. B. T., Ed. 2009; pp 1-6.
2. Amidon, G. L.; Lennernas, H.; Shah, V. P.; Crison, J. R., A Theoretical Basis for a Biopharmaceutic Drug Classification - The Correlation of in-vitro Drug Product Dissolution and in-vivo Bioavailability. *Pharmaceutical Research* **1995**, 12, (3), 413-420.
3. Apu, A. S.; Pathan, A. H.; Shrestha, D.; Kibria, G.; Jalil, R. U., Investigation of In vitro Release Kinetics of Carbamazepine from Eudragit (R) RS PO and RL PO Matrix Tablets. *Trop. J. Pharm. Res.* **2009**, 8, (2), 145-152.
4. Leuner, C.; Dressman, J., Improving drug solubility for oral delivery using solid dispersions. *European Journal of Pharmaceutics and Biopharmaceutics* **2000**, 50, (1), 47-60.
5. Benet, L. Z., There are no useful CYP3A probes that quantitatively predict the in vivo kinetics of other CYP3A substrates and no expectation that one will be found. *Mol. Interv.* **2005**, 5, (2), 79-+.
6. Sun, Y.; Rui, Y.; Wenliang, Z.; Tang, X., Nimodipine semi-solid capsules containing solid dispersion for improving dissolution. *International Journal of Pharmaceutics* **2008**, 359, (1-2), 144-149.
7. Joshi, G. V.; Kevadiya, B. D.; Patel, H. A.; Bajaj, H. C.; Jasra, R. V., Montmorillonite as a drug delivery system: Intercalation and in vitro release of timolol maleate. *International Journal of Pharmaceutics* **2009**, 374, (1-2), 53-57.
8. Forster, A.; Hempenstall, J.; Rades, T., Characterization of glass solutions of poorly water-soluble drugs produced by melt extrusion with hydrophilic amorphous polymers. *J. Pharm. Pharmacol.* **2001**, 53, (3), 303-315.
9. Yang, M.; Wang, P.; Huang, C.-Y.; Ku, M. S.; Liu, H.; Gogos, C., Solid dispersion of acetaminophen and poly(ethylene oxide) prepared by hot-melt mixing. *International Journal of Pharmaceutics* **2010**, 395, (1-2), 53-61.

10. Ha, J. U.; Xanthos, M., Novel delivery systems by melt compounding polymers with drug functionalized nanoclays. *Proc. 68th Annual Technical Conference Society of Plastics Engineers* **2010**, 56, 1193-1197.
11. Aguzzi, C.; Cerezo, P.; Viseras, C.; Caramella, C., Use of clays as drug delivery systems: Possibilities and limitations. *Applied Clay Science* **2007**, 36, (1-3), 22-36.
12. Viseras, C.; Cerezo, P.; Sanchez, R.; Salcedo, I.; Aguzzi, C., Current challenges in clay minerals for drug delivery. *Applied Clay Science* **2010**, 48, (3), 291-295.
13. Zhang, H.; Zou, K.; Guo, S.; Duan, X., Nanostructural drug-inorganic clay composites: Structure, thermal property and in vitro release of captopril-intercalated Mg-Al-layered double hydroxides. *Journal of Solid State Chemistry* **2006**, 179, (6), 1792-1801.
14. Xia, S.-J.; Ni, Z.-M.; Xu, Q.; Hu, B.-X.; Hu, J., Layered double hydroxides as supports for intercalation and sustained release of antihypertensive drugs. *Journal of Solid State Chemistry* **2008**, 181, (10), 2610-2619.
15. Zheng, J. P.; Luan, L.; Wang, H. Y.; Xi, L. F.; Yao, K. D., Study on ibuprofen/montmorillonite intercalation composites as drug release system. *Applied Clay Science* **2007**, 36, (4), 297-301.
16. Lin, F. H.; Lee, Y. H.; Jian, C. H.; Wong, J.-M.; Shieh, M.-J.; Wang, C.-Y., A study of purified montmorillonite intercalated with 5-fluorouracil as drug carrier. *Biomaterials* **2002**, 23, (9), 1981-1987.
17. Meng, N.; Zhou, N.-L.; Zhang, S.-Q.; Shen, J., Controlled release and antibacterial activity chlorhexidine acetate (CA) intercalated in montmorillonite. *International Journal of Pharmaceutics* **2009**, 382, (1-2), 45-49.
18. Marsac, P.; Li, T.; Taylor, L., Estimation of Drug-Polymer Miscibility and Solubility in Amorphous Solid Dispersions Using Experimentally Determined Interaction Parameters. *Pharmaceutical Research* **2009**, 26, (1), 139-151.
19. Minghetti, P.; Cilurzo, F.; Casiraghi, A.; Montanari, L., Application of viscometry and solubility parameters in miconazole patches development. *International Journal of Pharmaceutics* **1999**, 190, (1), 91-101.
20. Fedors, R. F., A method for estimating both the solubility parameters and molar volumes of liquids. *Polymer Engineering & Science* **1974**, 14, (2), 147-154.

21. Ghebremeskel, A. N.; Vemavarapu, C.; Lodaya, M., Use of surfactants as plasticizers in preparing solid dispersions of poorly soluble API: Selection of polymer-surfactant combinations using solubility parameters and testing the processability. *International Journal of Pharmaceutics* **2007**, 328, (2), 119-129.
22. Greenhalgh, D. J.; Williams, A. C.; Timmins, P.; York, P., Solubility parameters as predictors of miscibility in solid dispersions. *Journal of Pharmaceutical Sciences* **1999**, 88, (11), 1182-1190.
23. Albers, J.; Alles, R.; Matth e, K.; Knop, K.; Nahrup, J. S.; Kleinebudde, P., Mechanism of drug release from polymethacrylate-based extrudates and milled strands prepared by hot-melt extrusion. *European Journal of Pharmaceutics and Biopharmaceutics* **2009**, 71, (2), 387-394.
24. Mididoddi, P. K.; Repka, M. A., Characterization of hot-melt extruded drug delivery systems for onychomycosis. *European Journal of Pharmaceutics and Biopharmaceutics* **2007**, 66, (1), 95-105.
25. Rui, Y.; Yanjiao, W.; Xin, Z.; Jia, M.; Xing, T.; Xuefeng, Z., Preparation and Evaluation of Ketoprofen Hot-Melt Extruded Enteric and Sustained-Release Tablets. *Drug Development & Industrial Pharmacy* **2008**, 34, (1), 83-89.
26. Kakran, M.; Sahoo, N. G.; Li, L.; Judeh, Z., Dissolution of artemisinin/polymer composite nanoparticles fabricated by evaporative precipitation of nanosuspension. *J. Pharm. Pharmacol.* **2010**, 62, (4), 413-421.
27. Joshi, G. V.; Kevadiya, B. D.; Bajaj, H. C., Controlled release formulation of ranitidine-containing montmorillonite and Eudragit (R) E-100. *Drug Development and Industrial Pharmacy* **2010**, 36, (9), 1046-1053.
28. Li, B.; He, J.; Evans, D. G.; Duan, X., Enteric-coated layered double hydroxides as a controlled release drug delivery system. *International Journal of Pharmaceutics* **2004**, 287, (1-2), 89-95.
29. Han, Y. S.; Lee, S. Y.; Yang, J. H.; Hwang, H. S.; Park, I., Paraquat release control using intercalated montmorillonite compounds. *J. Phys. Chem. Solids* **2010**, 71, (4), 460-463.
30. Park, J. K.; Bin Choy, Y.; Oh, J. M.; Kim, J. Y.; Hwang, S. J.; Choy, J. H., Controlled release of donepezil intercalated in smectite clays. *International Journal of Pharmaceutics* **2008**, 359, (1-2), 198-204.

31. Chang, D. J.; Lamothe, M.; Stevens, R. M.; Sigal, L. H., Dapsone in rheumatoid arthritis. *Seminars in Arthritis and Rheumatism* **1996**, 25, (6), 390-403.
32. Rice, Z.; Bergkvist, M., Adsorption characteristics of a cationic porphyrin on nanoclay at various pH. *Journal of Colloid and Interface Science* **2009**, 335, (2), 189-195.
33. Riedel, A.; Leopold, C. S., Degradation of Omeprazole Induced by Enteric Polymer Solutions and Aqueous Dispersions: HPLC Investigations. *Drug Development and Industrial Pharmacy* **2005**, 31, (2), 151 - 160.
34. Schilling, S. U.; Shah, N. H.; Waseem Malick, A.; McGinity, J. W., Properties of melt extruded enteric matrix pellets. *European Journal of Pharmaceutics and Biopharmaceutics* **2010**, 74, (2), 352-361.
35. Patel, H.; Somani, R.; Bajaj, H.; Jasra, R., Nanoclays for polymer nanocomposites, paints, inks, greases and cosmetics formulations, drug delivery vehicle and waste water treatment. *Bulletin of Materials Science* **2006**, 29, (2), 133-145.
36. Joshi, G. V.; Kevadiya, B. D.; Bajaj, H. C., Design and evaluation of controlled drug delivery system of buspirone using inorganic layered clay mineral. *Microporous and Mesoporous Materials* **2010**, 132, (3), 526-530.
37. Vukovic, G. D.; Tomic, S. Z.; Marinkovic, A. D.; Radmilovic, V.; Uskokovic, P. S.; Colic, M., The response of peritoneal macrophages to dapsone covalently attached on the surface of carbon nanotubes. *Carbon* **2010**, 48, (11), 3066-3078.
38. Bruce, L. D.; Shah, N. H.; Waseem Malick, A.; Infeld, M. H.; McGinity, J. W., Properties of hot-melt extruded tablet formulations for the colonic delivery of 5-aminosalicylic acid. *European Journal of Pharmaceutics and Biopharmaceutics* **2005**, 59, (1), 85-97.
39. Cai, Y.; Hu, Y.; Song, L.; Xuan, S.; Zhang, Y.; Chen, Z.; Fan, W., Catalyzing carbonization function of ferric chloride based on acrylonitrile-butadiene-styrene copolymer/organophilic montmorillonite nanocomposites. *Polymer Degradation and Stability* **2007**, 92, (3), 490-496.
40. Gong, C.; Guan, R.; Shu, Y.-C.; Chuang, F.-S.; Tsen, W.-C., Effect of sulfonic group on solubility parameters and solubility behavior of poly(2,6-dimethyl-1,4-phenylene oxide). *Polymers for Advanced Technologies* **2007**, 18, (1), 44-49.